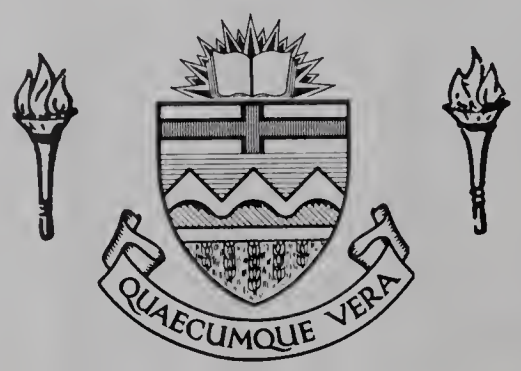

The University of Alberta
Printing Department
Edmonton, Alberta

THE UNIVERSITY OF ALBERTA

ICE FORMATION IN VERTICAL TUBES WITH CONVECTIVE BOUNDARY CONDITIONS

by

© ROBERT D.J. FREEBORN, B.Sc. (ALBERTA)

A THESIS

SUBMITTED TO THE FACULTY OF GRADUATE STUDIES

IN PARTIAL FULFILMENT OF THE REQUIREMENTS FOR THE DEGREE

OF MASTER OF SCIENCE

DEPARTMENT OF MECHANICAL ENGINEERING

EDMONTON, ALBERTA

SPRING, 1969

UNIVERSITY OF ALBERTA

FACULTY OF GRADUATE STUDIES

The undersigned certify that they have read, and recommend to the Faculty of Graduate Studies for acceptance, a thesis entitled "ICE FORMATION IN VERTICAL TUBES WITH CONVECTIVE BOUNDARY CONDITIONS" submitted by ROBERT D.J. FREEBORN in partial fulfilment of the requirements for the degree of Master of Science.

ABSTRACT

A theoretical and experimental investigation is presented for the problem of the transient growth of a frozen shell of ice that develops when superheated water flows through a vertical cylinder, whose wall is cooled convectively to a temperature below the freezing temperature. The solution of the theoretical problem is developed from the asymptotic solution for the temperature distribution in the ice, with prescribed convection as the boundary condition. This analysis was broken into two parts; a zone which is ice-free and a zone in which the ice formation takes place. The experimental results obtained agree well with the corresponding theoretical results in the region where the theory is applicable.

ACKNOWLEDGEMENTS

The author wishes to thank the following for their contributions.

- Dr. G.S.H. Lock for supervising the thesis,
- Mr. B. Bradbury who assembled the experimental apparatus and members of the Mechanical Engineering Shop who aided in the construction,
- Miss H. Wozniuk for typing the thesis,
- the National Research Council for the funds made available under Grant No. A-1672,
- my wife, Rene, for her patience and understanding during the last two years.

TABLE OF CONTENTS

TABLE OF CONTENTS (continued)

LIST OF FIGURES

NOMENCLATURE

a,r,η	radial displacement
α	thermal diffusivity
Bi_c	Biot number $(\frac{h_0 r_0}{k_i})$
c_p	specific heat
δ,ε	position of interface in freezing zone
Gr	Grashof number
h_0	convective heat transfer coefficient of coolant
k	thermal conductivity
ℓ	length of tube
λ	eigenvalue
L	latent heat of fusion
Nu_c	Nusselt number $(\frac{r_0 h_0}{k_\ell})$
ν	kinematic viscosity
p	pressure
Pe	Peclet number (PrRe)
Pr	Prandtl number
Q	volumetric flow rate
ρ	density
R	eigenfunction
Ra	Rayleigh number (GrPr)
Re	Reynolds number
r_p	variable in transient freezing problem
Ste	Stefan number $(\frac{c_p \theta_c}{L})$

σ	superheat ratio $(\frac{T_0 - T_f}{T_f - T_c})$
t, τ	time
T,θ,ϕ,Φ	temperature
u,v,V,U	velocity
x	variable in ice-free zone
χ	variable in energy equation (liquid)
z	axial length

SUBSCRIPTS

c	coolant, characteristic quantities in normalized equations
w	wall
0	tube inlet
ℓ	water
f	freezing
i	ice
z	axial direction
r	radial direction
s	steady state
d	based on diameter
e	entrance to the freezing zone
ro	based on radius of tube

SUPERSCRIPTS

*	freezing zone
+	ice-free zone
-	mean value

CHAPTER I

INTRODUCTION

Transient solidification of a superheated liquid flowing through a tube, whose wall temperature is lowered below that of the liquid freezing temperature, has a complicated history. As the liquid undergoes a change to the solid phase, thermal energy in the form of the latent heat of fusion is released from the moving solid-liquid interface where, in addition, heat may be removed from the flowing liquid.

This type of solidification problem arises in many familiar and important circumstances: for example; a buried pipe in a region of sporadic permafrost, the casting of metals, and freezing of foods. In some circumstances the tube wall may be cooled convectively, e.g. a water line exposed to a "cold" meteorological environment. Another area where problems of this type arise is in space technology. An example is provided by the hydraulic lines of space satellites which may be subjected to extreme environmental temperatures; if proper precautions are not taken solidification may occur. Yet another instance is in propulsion devices that utilize liquid-liquid heat exchangers in which one liquid is below the freezing temperature of the other: if the flow rate or the temperature of the "warm" liquid is low enough, a frozen layer will form on the exchanger walls.

A survey of the literature reveals that little information is available on the solidification of a liquid flowing through a tube with a convective boundary condition at the moving interface or a convective

boundary condition at the tube wall. Brush [1]* discussed the principles governing the freezing of water in mains. He presented no theoretical or experimental data but suggested that the formation of ice in water mains is dependent upon the temperature of the water and its flow rate as well as on the wall temperature.

London and Seban [2] describe a general approximate method for the solution of the one-coordinate freezing problem with application to the ice formation within various geometrical boundaries. Their analytical solutions were obtained from the construction of a thermal circuit, considering the sensible heat negligible relative to the latent heat of fusion of the liquid. They presented graphic and algebraic solutions for ice formation at spherical, cylindrical and plane boundaries along with an investigated degree of approximation of these solutions. It was shown that the analytical predictions of freezing times were comparable to those obtained experimentally.

Kreith and Romie [3] presented solutions for determining the position of the solid-liquid interface by considering the limited condition of a constant fusion velocity for cylinders and spheres with the water initially at the fusion temperature.

Stephenson [4] studied the problem of water flowing through a pipe exposed to an environment at temperatures below the freezing point. He presented an empirical equation, using thermal resistances, to relate three parameters of the problem; minimum mass flow rate required for ice

---

*Numbers in brackets denote references on page 68.

not to form, temperature of the water entering the exposed pipe, and resistance to heat transfer from the water to the environment.

Zerkle and Sunderland [5] discussed the effect of liquid solidification at the inner surface of a horizontal circular tube upon steady laminar flow heat transfer: they assumed steady state conditions, i.e. neglected latent heat effects. They found that, as could be expected, the amount of growth of the solid-liquid interface is dependent on the amount of superheat in the liquid and its flow rate. Their experiments were carried out with water in horizontal tubes and it was found that free convection produced considerable deviations from the theoretical results which ignored free convection.

Beaubouef and Chapman [6] analyzed the freezing of a solid phase from a fluid flowing past a "cold" surface. A finite-difference technique was employed to determine the thickness of the solid phase deposited by the flowing liquid, as a function of time and location on the surface.

Savino and Siegel [7] presented analytical predictions and experimental data for the transient growth of a frozen layer which forms when a flowing warm liquid is in contact with a plane wall that is cooled convectively from the opposite side. Three analytical procedures were employed and compared for accuracy and convenience in application; one of these is an iterative technique. Experimental values of ice thickness and plate surface temperature obtained throughout the transient growth period compared favorably with the theoretically predicted values.

Gort [8] studied the problem of freezing inside a long vertical cylinder with and without a forced internal flow. The theoretical solution which he used is an approximate solution for arbitrary departures of the cylinder wall temperature beneath the freezing temperature, with the fluid at its freezing temperature. Experimental work on this Dirichlet problem was conducted for no-flow and flow cases with particular emphasis on the influence of flow (and superheat) on the ice formation studied.

The recent work of Des Ruisseaux and Zerkle [9] is an extension of the work of Zerkle and Sunderland [5] where a theoretical technique is developed for predicting conditions under which a hydraulic system freezes shut. System pressure drop as a function of Reynolds number at steady-state conditions was determined analytically for various uniform wall temperatures. The theoretical results indicate a minimum pressure drop which should be maintained across a system to prevent it from freezing shut.

Very recently, Özisik and Mulligan [14] presented an analytical investigation of the transient freezing of a liquid flowing in a circular tube under the assumption of a constant wall temperature which is lower than the liquid freezing temperature: constant properties, a slug-flow velocity profile and quasi-steady state heat conduction in the solid phase were assumed. The method of solution involved the determination of an expression for the dimensionless temperature of both the solid and liquid phases in terms of the unknown solid-liquid interface radius. These expressions are coupled through the heat balance at the interface resulting

in a single ordinary differential equation for the interface radius. The analysis presented the variation of the local heat flux and the solid-liquid interface profile during freezing as a function of time and position along the tube. The analysis produced steady state heat transfer rates and axial profiles which were compared with the results of Zerkle and Sunderland.

The purpose of this thesis is to study the problem of transient freezing in a long vertical cylinder with a forced internal flow. An approximate theoretical solution for the interface history includes the convective heat transfer condition imposed at the inward moving interface of the frozen layer. The analysis is also concerned with a convective boundary condition on the outside of the cylinder wall, whose temperature is below the freezing point. Over an initial length of the cylinder the cooling is insufficient to cause solidification and therefore an ice-free zone exists. From this point on, ice grows radially inwards at a rate which is found to increase with the distance along the tube. The theoretical results are used to show how the ice thickness and pressure drop vary with length.

Representative experimental results are compared with the theoretical predictions and indicate the accuracy and range of validity of the theory.

PART I

THEORETICAL ANALYSIS

CHAPTER II

SOLUTION OF THE ICE-FREE PROBLEM

2.1 Governing Equations

Consider superheated water flowing vertically upwards in steady laminar motion, occupying the cylindrical domain shown in Figure 2.1. The water is assumed to have a uniform temperature and a fully developed velocity profile at the thermal entrance, i.e. $z = 0$. A prescribed convective boundary condition is applied at the wall of the cylinder, above $z = 0$, for times greater than zero. The tube wall has negligible thermal resistance in the cooling region.

The approximate form of the differential equation governing heat conduction in the water downstream from the thermal entrance, with radial symmetry and no sources, is given by

$$\frac{\partial^2 T_\ell}{\partial r^2} + \frac{1}{r}\frac{\partial T_\ell}{\partial r} = \frac{1}{\alpha_\ell}\left(v_z \frac{\partial T_\ell}{\partial z} + v_r \frac{\partial T_\ell}{\partial r}\right) \qquad 2.1\text{-}1$$

Boundary conditions (including convective cooling) may be written

$$\left(\frac{\partial T_\ell}{\partial r}\right)_{r=0} = 0$$

$$-k_\ell \left(\frac{\partial T_\ell}{\partial r}\right)_{r=r_0} = h_0(T_w - T_c)$$

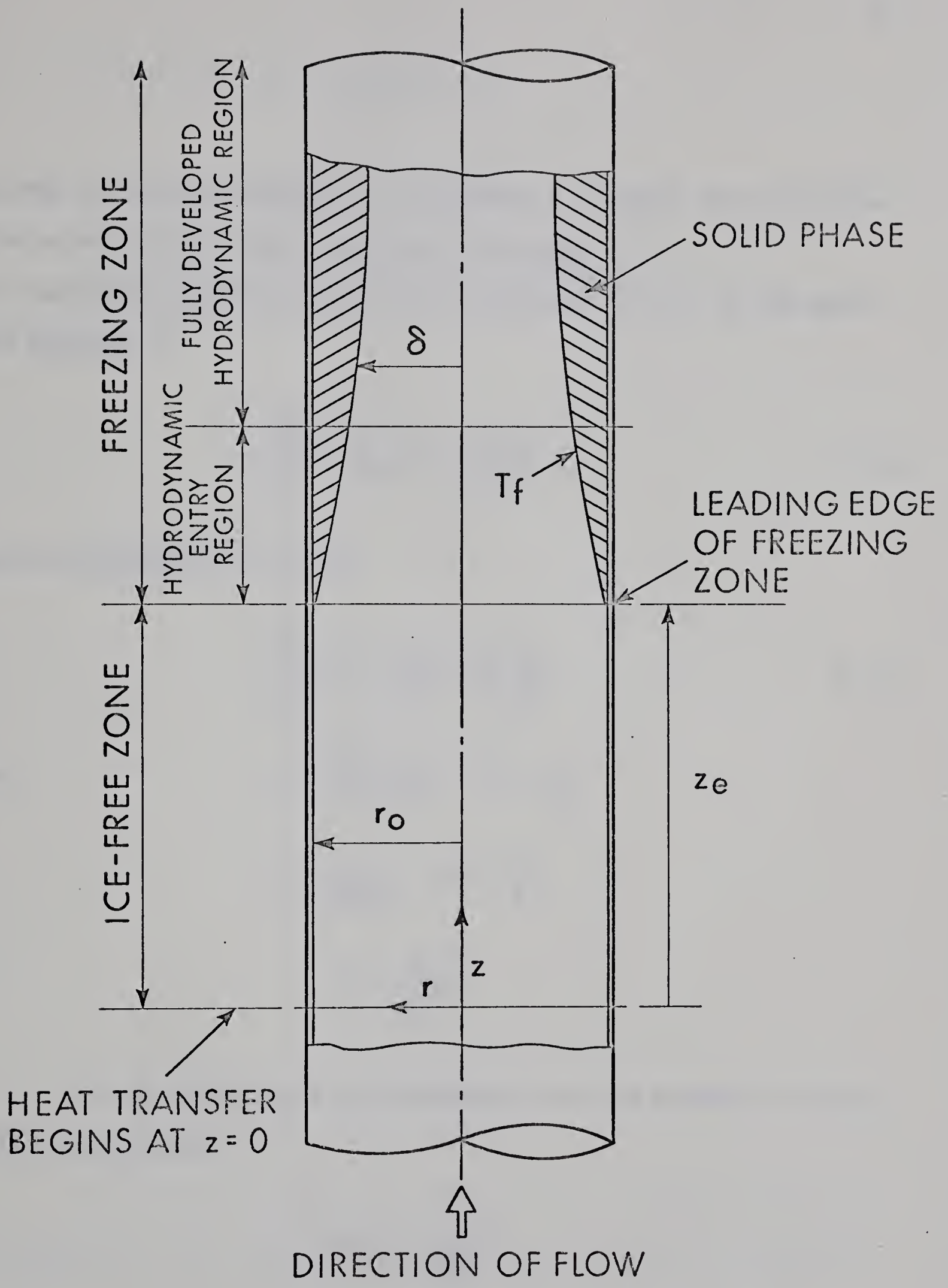

FIGURE 2.1 COORDINATE SYSTEM OF A TUBE WITH SOLIDIFICATION

$$T_\ell(r,0) = T_0$$

(An order of magnitude analysis - see Appendix B - reveals that conduction in the axial direction may be neglected since $\frac{1}{PrRe} << 1$).

With the velocity profile assumed fully developed, i.e. $v_r = 0$, the applicable equation is

$$\frac{\partial^2 T_\ell}{\partial r^2} + \frac{1}{r}\frac{\partial T_\ell}{\partial r} = \frac{v_z}{\alpha_\ell}\frac{\partial T_\ell}{\partial z} \qquad 2.1\text{-}2$$

Normalizing equation 2.1-2 gives

$$\frac{\partial^2 \Phi_\ell}{\partial r^{+2}} + \frac{1}{r^+}\frac{\partial \Phi_\ell}{\partial r^+} = \frac{u^+}{2}\frac{\partial \Phi_\ell}{\partial z^+} \qquad 2.1\text{-}3$$

where $$\Phi_\ell = \frac{T_\ell - T_c}{T_0 - T_c}, \quad r^+ = \frac{r}{r_0}$$

$$z^+ = \frac{z}{r_0 Pe_d}, \quad u^+ = \frac{v_z}{V}$$

$$V = \frac{Q}{\pi r_0^2}$$

For hydrodynamically fully developed flow the parabolic velocity profile is applicable

$$v_z = 2V[1 - (\frac{r}{r_0})^2]$$

Normalizing yields

$$u^+ = 2(1 - r^{+2}) \qquad 2.1\text{-}4$$

Substituting into equation 2.1-2, the final form of the differential equation is

$$\frac{\partial^2 \Phi_\ell}{\partial r^{+2}} + \frac{1}{r^+}\frac{\partial \Phi_\ell}{\partial r^+} = (1 - r^{+2})\frac{\partial \Phi_\ell}{\partial z^+} \qquad 2.1\text{-}5$$

The boundary conditions then are

$$\left(\frac{\partial \Phi_\ell}{\partial r^+}\right)_{r^+=0} = 0$$

$$\left(\frac{\partial \Phi_\ell}{\partial r^+}\right)_{r^+=1} = -\mathrm{Nu}_c \Phi_w$$

$$\Phi_\ell(r^+,0) = 1$$

where $$\mathrm{Nu}_c = \frac{r_0 h_0}{k_\ell}$$

$$\Phi_w = \frac{T_w - T_c}{T_0 - T_c}$$

Equation 2.1-5 and the succeeding boundary conditions are linear and homogeneous, and as such can be solved using the method of separation

of variables by taking

$$\Phi_{\ell}(r^+,z^+) = R(r^+)\cdot Z(z^+) \ . \qquad 2.1\text{-}6$$

This leads to two ordinary differential equations†

$$Z' + \lambda^2 Z = 0 \qquad 2.1\text{-}7$$

$$R'' + \frac{1}{r^+} R' + \lambda^2 R(1 - r^{+2}) = 0 \ . \qquad 2.1\text{-}8$$

The first of these is satisfied by an exponential function, i.e. $Z = C \exp(- \lambda^2 z^+)$. The second equation is of the Sturm-Liouville type, where the solutions that satisfy the boundary conditions can be found for an infinite number of eigenvalues λ. That is

$$R(r^+) = AR_1(r^+) + BR_2(r^+).$$

Yielding

$$\Phi_{\ell}(r^+,z^+) = [AR_1(r^+) + BR_2(r^+)]\ C \exp(- \lambda^2 z^+) \ .$$

Application of the boundary conditions leads to

$$B = 0$$

---

†$'$, $''$ first and second derivatives with respect to the argument

$$\frac{1}{Nu_c} + \frac{R_1(r^+)}{R_1'(r^+)}\Big|_{r^+=1} = 0 \qquad 2.1\text{-}9$$

Thus the solution of equation 2.1-5 may be written in the form

$$\Phi_\ell(r^+,z^+) = \sum_{n=0}^{\infty} c_n\, R_n(r^+) \exp\,(-\lambda_n{}^2 z^+) \qquad 2.1\text{-}10$$

where λ_n are the roots of the transcendental equation and $R_n(r^+)$ are the eigenfunctions corresponding to the function $R_1(r^+)$. Applying the initial condition the coefficients c_n are determined by the relation [15]

$$c_n = \frac{\int_0^1 r^+(1-r^{+2})\, R_n(r^+)\, dr^+}{\int_0^1 r^+(1-r^{+2})\, R_n{}^2(r^+)\, dr^+} \qquad 2.1\text{-}11$$

since $R_n(r^+)$ is an orthonormal function.

Following the work of Sellars, Tribus and Klein [10], the solution of equation 2.1-8 is sought for higher eigenvalues. This was accomplished by obtaining an asymptotic solution for equation 2.1-8 for $\lambda_n \to \infty$. The resulting equation for $R(r^+)$ is the WKB approximation and is valid for $0 < r^+ < 1$ and large λ. Examination of equation 2.1-8 shows that when r^+ is very small, i.e. $\lambda^2(1 - r^{+2}) \to \lambda^2$, the classical solution behaves as a Bessel function of zero order of the first kind: thus $R(r^+) = J_0(\lambda r^+)$. For large λr^+, the asymptotic solution for $J_0(\lambda r^+)$ is matched to the WKB approximation to determine the coefficients of the latter for r^+

small. Since the resulting solution has a singularity at $r^+ \to 1$, an alternate solution is required because a boundary condition is to be imposed at $r^+ = 1$. This is accomplished by making a change of variable, i.e. $x^+ = 1 - r^+$, and substituting into equation 2.1-8 for small x^+. Yet another substitution of a new variable yields, for large λ, a differential equation which results in a further solution to equation 2.1-8. This new solution is matched to the previously obtained solution to evaluate the formers' unknown constants. The above procedure thus provides a solution valid for small x^+ (near the wall). The solution is [10]

$$R(x^+) = \frac{2}{3}\sqrt{2x^+}\left[\sin\left(\frac{\lambda\pi}{4} - \frac{\pi}{3}\right) J_{\frac{1}{3}}\left(\frac{\lambda\sqrt{8}\ x^{+3/2}}{3}\right)\right.$$

$$\left. - \sin\left(\frac{\lambda\pi}{4} - \frac{2\pi}{3}\right) J_{-\frac{1}{3}}\left(\frac{\lambda\sqrt{8}\ x^{+3/2}}{3}\right)\right] \qquad 2.1\text{-}12$$

2.2 Eigenvalues

From equation 2.1-12 the ratio $\left.\frac{R(r^+)}{R'(r^+)}\right|_{r^+=1}$ is found to be

$$\left.\frac{R(r^+)}{R'(r^+)}\right|_{r^+=1} = R(x^+)/ - \left.\frac{\partial R(x^+)}{\partial x^+}\right|_{x^+=0}$$

$$= \frac{3^{\frac{2}{3}}\,\Gamma\left(\frac{4}{3}\right)\sin\left(\frac{\lambda\pi}{4} - \frac{2\pi}{3}\right)}{2^{\frac{1}{3}}\,\Gamma\left(\frac{2}{3}\right)\lambda^{\frac{2}{3}}\sin\left(\frac{\lambda\pi}{4} - \frac{\pi}{3}\right)} \qquad 2.2\text{-}1$$

This may now be substituted into the convective boundary condition

(equation 2.1-9) resulting in the transcendental equation.

$$\frac{1}{Nu_c} + \frac{3^{\frac{2}{3}}\,\Gamma(\frac{4}{3})\,\sin\,(\frac{\lambda\pi}{4} - \frac{2\pi}{3})}{2^{\frac{1}{3}}\,\Gamma(\frac{2}{3})\,\lambda^{\frac{2}{3}}\,\sin\,(\frac{\lambda\pi}{4} - \frac{\pi}{3})} = 0 \qquad 2.2\text{-}2$$

This equation leads to an infinite set of eigenvalues, each set depending on the choice of Nusselt number Nu_c. As $Nu_c \to \infty$, the eigenvalues tend to those obtained by Sellars, et al [10] since the boundary condition then becomes a Dirichlet type, i.e. a constant wall temperature, in which case it is evident that $\lambda_n = 4n + \frac{8}{3}$.

2.3 Ice-Free Length

Once the eigenvalues have been determined from the boundary condition at the wall, the length of the ice-free zone, z_e^+, may be determined. This is found from equation 2.1-10 such that

$$\Phi_\ell(1,\, z_e^+) = \Phi_e = \frac{T_f - T_c}{T_0 - T_c}\,.$$

At this point, where the wall temperature is at the freezing temperature, the corresponding temperature profile must be calculated again using equation 2.1-10. This temperature profile will become the input profile to the freezing zone.

The theoretical results are shown graphically in Figure 2.2 which demonstrates the variation in the length of the ice-free zone versus superheat ratio $[\sigma = (T_0 - T_f)/(T_f - T_c)]$ for various Biot

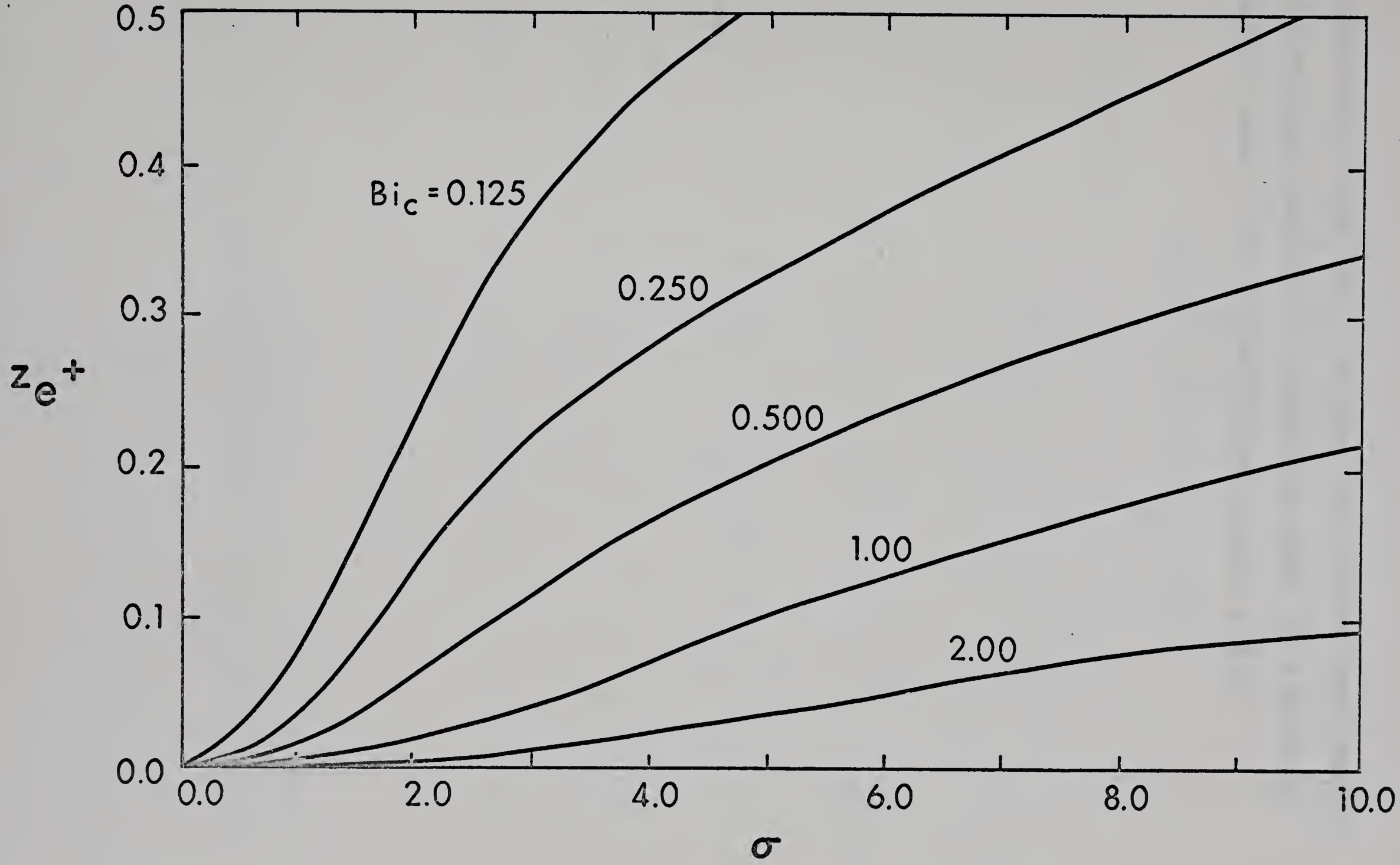

FIGURE 2.2 VARIATION OF z_e^+ WITH SUPERHEAT RATIO

numbers [$Bi_c = (k_\ell/k_i)\ Nu_c$]. As shown, the ice-free length decreases with decreased superheat or increased Biot number for a particular Reynolds number. This verifies what was expected a priori.

CHAPTER III

SOLUTION OF THE FREEZING PROBLEM

3.1 Governing Equations

This chapter is concerned with the transient freezing of water flowing vertically upwards in steady laminar motion through a cylindrical tube with solidification at the inner wall surface. Consider the flowing water and its corresponding ice shell occupying the cylindrical domain shown in Figure 2.1. The superheated water now has a modified temperature profile at the leading edge of the freezing zone due to cooling in the ice-free zone. Since the water is cooled further as it flows through the freezing zone, its mean temperature approaches the freezing temperature and the thickness of the ice shell increases. Due to this variation in the cross-section a two-dimensional velocity distribution is produced.

Assuming the ice properties constant, the conduction equation within the ice layer, with radial symmetry and no sources, is given by

$$\frac{\partial^2 T_i}{\partial r^2} + \frac{1}{r}\frac{\partial T_i}{\partial r} = \frac{1}{\alpha_i}\frac{\partial T_i}{\partial t} \qquad 3.1\text{-}1$$

Where axial conduction has been shown by an order of magnitude analysis (Appendix B) to be negligible. The system is subject to the following initial and boundary conditions

$$T_i(\delta,t) = T_f$$

$$-k_i\left(\frac{\partial T_i}{\partial r}\right)_{r=r_0} = h_0(T_w - T_c)$$

$$T_i(r_0,0) = T_f$$

The temperature distribution in the liquid downstream from the entrance to the freezing zone is described by the energy equation

$$v_r \frac{\partial T_\ell}{\partial r} + v_z \frac{\partial T_\ell}{\partial z} = \alpha_\ell\left[\frac{1}{r}\frac{\partial}{\partial r}\left(r \frac{\partial T_\ell}{\partial r}\right)\right] \qquad 3.1\text{-}2$$

With the corresponding boundary conditions

$$T_\ell(r,0) = T_0$$

$$T_\ell(\delta,z) = T_f$$

$$\left(\frac{\partial T_\ell}{\partial r}\right)_{r=0} = 0$$

Conservation of mass is represented by

$$\frac{1}{r}\frac{\partial(rv_r)}{\partial r} + \frac{\partial v_z}{\partial z} = 0 \qquad 3.1\text{-}3$$

or

$$2\pi \int_0^\delta v_z\, r\, dr = Q$$

Taking as an approximation

$$v_z(r,z) = 2V\left(\frac{r_0}{\delta}\right)^2 \left[1 - \left(\frac{r}{\delta}\right)^2\right] \qquad 3.1\text{-}4$$

and using equations 3.1-3

$$v_r(r,z) = 2V \frac{r\, r_0^2}{\delta^3} \frac{d\delta}{dz} \left[1 - \left(\frac{r}{\delta}\right)^2\right]. \qquad 3.1\text{-}5$$

These equations imply that the flow cross section is slowly varying and reveal that $\frac{v_r}{v_z} << 1$ if $\frac{d\delta}{dz} << 1$. After substitution of the velocity components, equation 3.1-2 becomes

$$2V\left(\frac{r_0}{\delta}\right)^2 \left[1 - \left(\frac{r}{\delta}\right)^2\right]\left[\frac{r}{\delta} \frac{d\delta}{dz} \frac{\partial T_\ell}{\partial r} + \frac{\partial T_\ell}{\partial z}\right] = \alpha_\ell\left[\frac{1}{r} \frac{\partial}{\partial r} \left(r \frac{\partial T_\ell}{\partial r}\right)\right]. \qquad 3.1\text{-}6$$

Following Zerkle and Sunderland [5], the above equation is normalized, yielding

$$\frac{1}{\delta^{*2}} \left[1 - \left(\frac{r^*}{\delta^*}\right)^2\right]\left[\frac{r^*}{\delta^*} \frac{d\delta^*}{dz^*} \frac{\partial \phi_\ell}{\partial r^*} + \frac{\partial \phi_\ell}{\partial z^*}\right] = \left[\frac{\partial^2 \phi_\ell}{\partial r^{*2}} + \frac{1}{r^*} \frac{\partial \phi_\ell}{\partial r^*}\right] \qquad 3.1\text{-}7$$

with the boundary conditions

$$\phi_\ell(r^*,0) = 1$$

$$\phi_\ell(\delta^*,z^*) = 0$$

$$\left(\frac{\partial \phi_\ell}{\partial r^*}\right)_{r^*=0} = 0$$

where $$\phi_\ell(r^*,z^*) = \frac{\theta_\ell}{\theta_{c\ell}}, \quad \theta_\ell = T_\ell - T_f, \quad \theta_{c\ell} = T_0 - T_f$$

$$r^* = \frac{r}{r_0}, \quad \delta^* = \frac{\delta}{r_0}, \quad z^* = \frac{z}{r_0 Pe_d} .$$

It should be emphasized at this point that the axial position is now measured from the leading edge of the freezing zone.

When the substitution, $\eta = \frac{r}{\delta}$, is used in equation 3.1-7, the resulting equation and boundary conditions are of the same form as the system describing the classical Graetz problem

$$(1 - \eta^2)\frac{\partial \phi_\ell}{\partial z^*} = \left[\frac{\partial^2 \phi_\ell}{\partial \eta^2} + \frac{1}{\eta}\frac{\partial \phi_\ell}{\partial \eta}\right] \qquad 3.1\text{-}8$$

and the corresponding boundary conditions

$$\phi_\ell(\eta,0) = 1$$

$$\phi_\ell(1,z^*) = 0$$

$$\left(\frac{\partial \phi_\ell}{\partial \eta}\right)_{\eta=0} = 0 .$$

The non-dimensional temperature distribution is then given by

$$\phi_\ell(\eta,z) = \sum_{j=0}^{\infty} c_j R_j(\eta) \exp(-\lambda_j^2 z^*) \qquad 3.1\text{-}9$$

with the temperature gradient at the ice-water interface given by

$$\left[-\frac{\partial \phi_{\ell}}{\partial \eta}(1,z^*)\right] = 2 \sum_{j=0}^{\infty} \left[-c_j R_j'(1)/2\right] \exp\left(-\lambda_j^2 z^*\right) \qquad 3.1\text{-}10$$

and the heat transfer by

$$q = \frac{2k_{\ell}(T_0-T_f)}{\delta} \sum_{j=0}^{\infty} \frac{c_j}{2} R_j'(1) \exp\left(-\lambda_j^2 z^*\right). \qquad 3.1\text{-}11$$

In the present problem, however, the values of the coefficient, c_j, cannot be taken from Sellars, et al [10] as done by Zerkle and Sunderland [5]. This is due to the fact that the temperature profile at the leading edge of the freezing zone is not a block profile but has been modified by convection in the ice-free zone. Thus we must write [15]

$$c_j = \frac{\int_0^1 \phi_{\ell}(\eta,0)\eta(1-\eta^2)R_j(\eta)d\eta}{\int_0^1 \eta(1-\eta^2)\, R_j^{\,2}(\eta)\, d\eta} \qquad 3.1\text{-}12$$

where

$$\phi_{\ell}(\eta,0) = \frac{(T_c-T_f) + (T_0-T_c) \sum_{n=0}^{\infty} c_n R_n(\eta) \exp\left(-\lambda_n^2 z_e^+\right)}{T_0 - T_f}$$

noting that at z_e^+, η is identically r^+.

Consider now the heat balance at the interface. The heat flux through the frozen layer to the cylinder wall is equal to the sensible heat extracted from the freezing fluid, together with the latent heat of

fusion released by the solidification process as the ice layer increases in thickness. The cylinder wall is assumed to have negligible thickness and therefore negligible thermal capacity and radial resistance.

The heat balance at the interface may thus be written

$$- k_\ell \left.\frac{\partial T_\ell}{\partial r}\right|_\delta - \rho_i L_i \frac{d\delta}{dt} = - k_i \left.\frac{\partial T_i}{\partial r}\right|_\delta \qquad 3.1\text{-}13$$

3.2 Solution for Steady State Conditions

When a superheated liquid is flowing through the freezing zone, the frozen shell of ice will eventually reach a steady state thickness for every axial position when, at the interface, the heat flux in the liquid is equal to the heat flux in the ice. The resulting steady state interface radius will be used as a reference in the later analysis and hence will be derived separately. It will be assumed that the temperature at the ice-water interface is constant and equal to the freezing temperature.

3.2-1 Temperature Distribution

The approximate form of the energy equation in the ice shell is

$$\frac{\partial^2 T_i}{\partial r^2} + \frac{1}{r}\frac{\partial T_i}{\partial r} = 0 \qquad 3.2\text{-}1.1$$

as revealed by the order of magnitude analysis in Appendix B. The appropriate boundary conditions are

$$- k_i \left(\frac{\partial T_i}{\partial r}\right)_{r=r_0} = h_0 (T_w - T_c)$$

$$T_i(\delta_s) = T_f \ .$$

Normalizing equation 3.2-1.1 we obtain

$$\frac{\partial^2 \phi_i}{\partial r^{*2}} + \frac{1}{r^*} \frac{\partial \phi_i}{\partial r^*} = 0$$

where $$\phi_i = \frac{\theta_i}{\theta_{ci}} \ , \ \theta_i = T_i - T_f \ , \ \theta_{ic} = T_f - T_c \ .$$

The solution of the reduced equation is well known and given by

$$\phi_i(r^*) = c(z) \ln r^* + D(z) \ . \qquad 3.2\text{-}1.2$$

The normalized boundary conditions are

$$\left(\frac{\partial \phi_i}{\partial r^*}\right)_{r^*=1} = - Bi_c \left[\phi_i(1) + 1\right]$$

$$\phi_i(\delta_s^*) = 0$$

where $$Bi_c = \frac{r_0 h_0}{k_i} \ , \ r^* = \frac{r}{r_0} \ , \ \delta_s^* = \frac{\delta_s}{r_0} \ .$$

If $\phi_i(1)$ is the normalized cylinder wall temperature, then the solution for the temperature in the ice shell is

$$\phi_i(r^*) = \phi_i(1)\left[1 - \frac{\ln r^*}{\ln \delta_s^*}\right] . \qquad 3.2\text{-}1.3$$

Using equation 3.2-1.3 and the convective boundary condition at the wall we find that

$$\phi_i(1) = \frac{Bi_c \ln \delta_s^*}{1 - Bi_c \ln \delta_s^*} \qquad 3.2\text{-}1.4$$

so that equation 3.2-1.3 becomes

$$\phi_i(r^*) = \frac{\ln \delta_s^* - \ln r^*}{\frac{1}{Bi_c} - \ln \delta_s^*} \qquad 3.2\text{-}1.5$$

3.2-2 Interface Location

The energy balance at the ice-water interface under steady state conditions is the same as equation 3.1-13 except that $\frac{d\delta}{dt} = 0$ since the interface has ceased to grow. Thus

$$-k_\ell \frac{\partial T_\ell}{\partial r}\Big|_{\delta_s} = -k_i \frac{\partial T_i}{\partial r}\Big|_{\delta_s} . \qquad 3.2\text{-}2.1$$

As seen from equation 3.1-11,

$$-k_\ell \frac{\partial T_\ell}{\partial r}\Big|_{\delta_s} = \frac{2k_\ell (T_0 - T_f)}{\delta_s} \sum_{j=0}^{\infty} \frac{c_j}{2} R_j'(1) \exp(-\lambda_j^2 z^*) .$$

Denoting $\chi = \sum_{j=0}^{\infty} \frac{c_j}{2} R_j'(1) \exp(-\lambda_j^2 z^*)$ equation 3.2-2.1 becomes

$$- k_i \frac{\partial T_i}{\partial r}\Big|_{\delta_s} = \frac{2k_\ell (T_0 - T_f)\chi}{\delta_s} \quad . \qquad 3.2\text{-}2.2$$

Substituting into equation 3.2-2.1 and normalizing we obtain

$$\frac{\partial \phi_i}{\partial r^*}\Big|_{\delta_s^*} = - \frac{2k_\ell}{k_i}\left(\frac{T_0 - T_f}{T_f - T_c}\right) \frac{\chi}{\delta_s^*}$$

$$= - \frac{2k_\ell}{k_i} \frac{\sigma\chi}{\delta_s^*} \qquad 3.2\text{-}2.3$$

where σ is the superheat ratio.

Substituting equation 3.2-1.5 yields

$$\ln \delta_s^* = \frac{1}{Bi_c} - \frac{1}{\beta} \qquad 3.2\text{-}2.4$$

where $$\beta = \frac{2k_\ell}{k_i} \sigma\chi \ .$$

Therefore

$$\delta_s^* = \exp\left(\frac{1}{Bi_c} - \frac{1}{\beta}\right) \quad . \qquad 3.2\text{-}2.5$$

It is worth mentioning that for the Dirichlet problem, i.e. $Bi_c \to \infty$ and the wall temperature constant, this result reduces to the result given by Zerkle and Sunderland [5], as expected.

3.3 Solution for Transient Conditions

3.3-1 Temperature Distribution

Consider the equation for the heat balance at the ice-water interface in the freezing zone as given by equation 3.1-13 but rewritten in the form

$$\frac{2k_{\ell}(T_0-T_f)\,\chi}{r}\Big|_{\delta} - \rho_i L_i \frac{d\delta}{dt} = - k_i \frac{\partial T_i}{\partial r}\Big|_{\delta}. \qquad 3.3\text{-}1.1$$

Considering radial displacement normally inward from the wall, i.e. $r' = r_0 - r$ and $\delta' = r_0 - \delta$, then the above equation becomes

$$\frac{2k_{\ell}\theta_{c\ell}\,\chi}{r_0 - r'}\Big|_{\delta'} + \rho_i L_i \frac{d\delta'}{dt} = k_i \frac{\partial T_i}{\partial r'}\Big|_{\delta'} . \qquad 3.3\text{-}1.2$$

Normalizing equation 3.3-1.2 will give

$$\frac{2k_{\ell}\theta_{c\ell}\,\chi}{r_0 - ar_c}\Big|_{\varepsilon} + \frac{\rho_i L_i r_c}{t_c} \frac{d\varepsilon}{d\tau} = \frac{k_i \theta_{ci}}{r_c} \frac{\partial \phi_i}{\partial a}\Big|_{\varepsilon} \qquad 3.3\text{-}1.3$$

where $a = \frac{r'}{r_c}$, $\varepsilon = \frac{\delta'}{r_c}$, $\phi_i = \frac{\theta}{\theta_{ci}}$, $\theta = T_i - T_f$, $\tau = \frac{t}{t_c}$.

Further rearrangement yields

$$\frac{2k_{\ell}\sigma\chi r_p}{k_i(1-r_p\varepsilon)} + \left[\frac{\rho_i L_i r_0^2 r_p^2}{t_c k_i \theta_{ci}}\right] \frac{d\varepsilon}{d\tau} = \frac{\partial \phi_i}{\partial a}\Big|_{\varepsilon} \qquad 3.3\text{-}1.4$$

where $r_c = r_0 - \delta_s$, $r_p = \frac{r_0 - \delta_s}{r_0}$, $\theta_{ci} = T_f - T_c$, $\sigma = \frac{\theta_{c\ell}}{\theta_{ci}}$.

Then

$$\frac{\partial \phi_i}{\partial a}\Big|_{\varepsilon} - \frac{r_p \beta}{1 - r_p \varepsilon} = \left[\frac{\rho_i L_i r_p^2 r_0^2}{k_i \theta_{ci} t_c}\right] \frac{d\varepsilon}{d\tau} \quad . \qquad 3.3\text{-}1.5$$

For a growing layer of ice the coefficient of the right hand term in equation 3.3-1.6 can not be very small without suppressing the nature of the problem, i.e. ice formation. Taking the coefficient identically equal to unity we define t_c as

$$t_c = \frac{1}{Ste} \left[\frac{\rho_i r_p^2 r_0^2 c_{pi}}{k_i}\right]$$

where $Ste = \frac{c_{pi} \theta_{ci}}{L_i}$ is the Stefan number, Lock [11]. This is the ratio of the sensible heat to the latent heat. The normalized interface equation is then

$$\frac{\partial \phi_i}{\partial \varepsilon} - \frac{r_p \beta}{1 - r_p \varepsilon} = \frac{d\varepsilon}{d\tau} \quad . \qquad 3.3\text{-}1.6$$

Normalizing the conduction equation for the ice shell in the freezing zone, as given by equation 3.1-1, in a similar fashion as shown previously we obtain

$$\frac{\partial^2 \phi_i}{\partial a^2} - \frac{r_p}{1 - r_p a} \frac{\partial \phi_i}{\partial a} = \left[\frac{(r_0 r_p)^2}{t_c \alpha_i}\right] \frac{\partial \phi_i}{\partial \tau}$$

Substituting for t_c, the normalized conduction equation becomes

$$\frac{\partial^2 \phi_i}{\partial a^2} - \frac{r_p}{1 - r_p a} \frac{\partial \phi_i}{\partial a} = \text{Ste} \frac{\partial \phi_i}{\partial \tau} \quad . \qquad 3.3\text{-}1.7$$

The normalized initial and boundary conditions are then

$$\phi_i(\varepsilon,\tau) = 0$$

$$\left(\frac{\partial \phi_i}{\partial a}\right)_{a=0} = r_p \text{Bi}_c \, [\phi_i(0,\tau) + 1] \qquad 3.3\text{-}1.8$$

$$\phi_i(1,\infty) = 0$$

where $\phi_i(0, \tau)$ is the normalized wall temperature.

For the problem under consideration the analysis will be restricted to Ste << 1, i.e. the latent heat effects dominates over the sensible heat effects. For an ice-water system the Stefan number is usually less than unity and may be very much less. For this reason, the ice interface advances very slowly inward which suggests a perturbation expansion in Ste itself. The solution of equation 3.3-1.7 is then taken as

$$\phi_i(a,\tau) = \phi_{io}(a,\tau) + \sum_{n=1}^{\infty} \text{Ste}^n \, \phi_{in}(a,\tau) \quad .$$

Substituting into equation 3.3-1.7 and grouping powers of Ste we obtain an infinite set of equations. Here we will only consider the asymptotic solution $\phi_{io}(a,\tau)$. For this analysis, we will call the temperature a "quasi-steady" solution since the steady state conduction equation is used. The temperature distribution is thus logarithmic at all times.

The "quasi-steady" temperature distribution is given by

$$\phi_{io}(a,\tau) = - \frac{A(\tau)}{r_p} \ln (1 - r_p a) + B(\tau) \ . \qquad 3.3\text{-}1.9$$

Using the boundary conditions (equations 3.3-1.8)

$$\phi_{io}(a,\tau) = \phi_{io}(0,\tau) \left[1 - \frac{\ln(1 - r_p a)}{\ln(1 - r_p \varepsilon)}\right] \qquad 3.3\text{-}1.10$$

where $\phi_{io}(0,\tau)$ is the normalized cylinder wall temperature given by

$$\phi_{io}(0,\tau) = \frac{Bi_c \ln(1 - r_p \varepsilon)}{1 - Bi_c \ln(1 - r_p \varepsilon)} \qquad 3.3\text{-}1.11$$

then

$$\phi_{io}(a,\tau) = \frac{Bi_c [\ln(1 - r_p \varepsilon) - \ln(1 - r_p a)]}{1 - Bi_c \ln(1 - r_p \varepsilon)} \ . \qquad 3.3\text{-}1.12$$

3.3-2 Interface Location

Using the zeroth approximation of the temperature solution in the interface equation 3.3-1.6 we obtain

$$\frac{d\varepsilon}{d\tau} = \frac{\partial \phi_{io}}{\partial r}\Big|_{\varepsilon} - \frac{r_p \beta}{1 - r_p \varepsilon} \qquad 3.3\text{-}2.1$$

or substituting equation 3.3-1.12 gives

$$\frac{d\varepsilon}{d\tau} = \left\{\frac{r_p \, Bi_c}{(1-r_p a)\,[1 - Bi_c \ln(1-r_p a)]}\Big|_{\varepsilon}\right\} - \frac{r_p \beta}{1 - r_p \varepsilon} \, . \qquad 3.3\text{-}2.2$$

Further rearrangement yields

$$\frac{d\varepsilon}{d\tau} = r_p \left\{\frac{1 - \beta\left[\frac{1}{Bi_c} - \ln(1-r_p\varepsilon)\right]}{(1-r_p\varepsilon)\left[\frac{1}{Bi_c} - \ln(1-r_p\varepsilon)\right]}\right\} \, . \qquad 3.3\text{-}2.3$$

It is evident that the solution of equation 3.3-2.3 will predict the interface history at any axial position for a given flow rate, superheat ratio and Biot number.

CHAPTER IV

SOLUTION OF THE MERGED PROBLEM

4.1 Interface Growth and Temperature Distribution

Numerical results were obtained for the theoretical analysis using an IBM 360/67 computer, in the Department of Computing Science, University of Alberta. Appendix A provides the program which determines the eigenvalues, eigenfunctions, the length of the ice-free zone, the temperature profile at the entrance to the freezing zone and the history of the interface at any point in the freezing zone. Axial profiles of ice thickness and pressure drop were also calculated. Representative results are shown graphically by Figures 4.1 and 4.2.

The eigenvalues of equation 2.2-2 were calculated to the desired accuracy by substituting an evaluated initial guess into a Newton-Raphson iterative technique. Equation 2.1-9 and the variable χ, which involve infinite series, were evaluated by summing the first forty terms. The integrals in equations 2.1-11 and 3.1-12 were evaluated by means of the Simpson rule, while the differential equations for determining the eigenfunctions and interface history (equations 2.1-8 and 3.3-2.3) were solved by a fourth-order Runge-Kutta method of forward integration.

In the analysis it was assumed that the properties of the ice and water were constant.

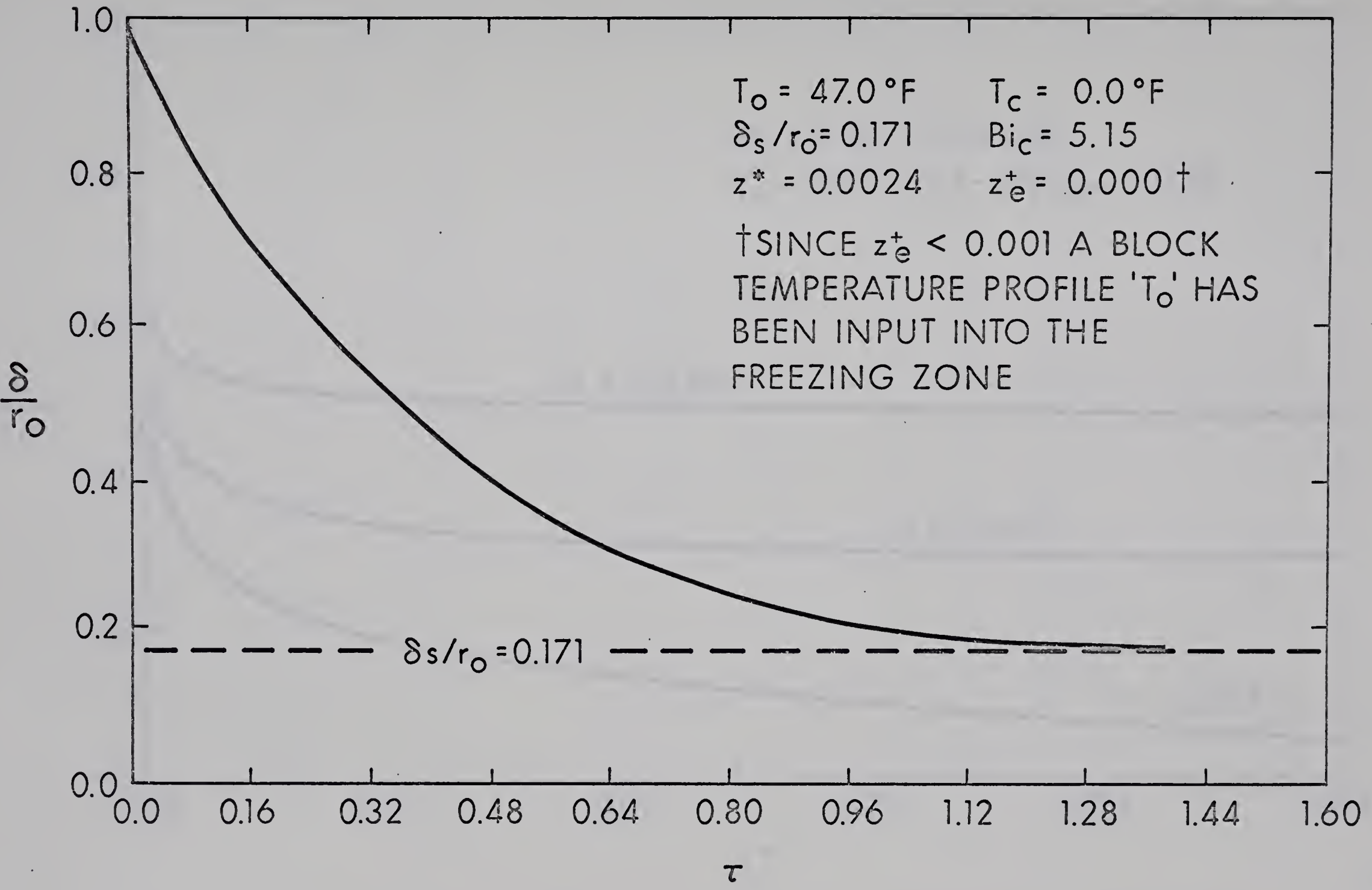

FIGURE 4.1 INTERFACE POSITION VS. TIME

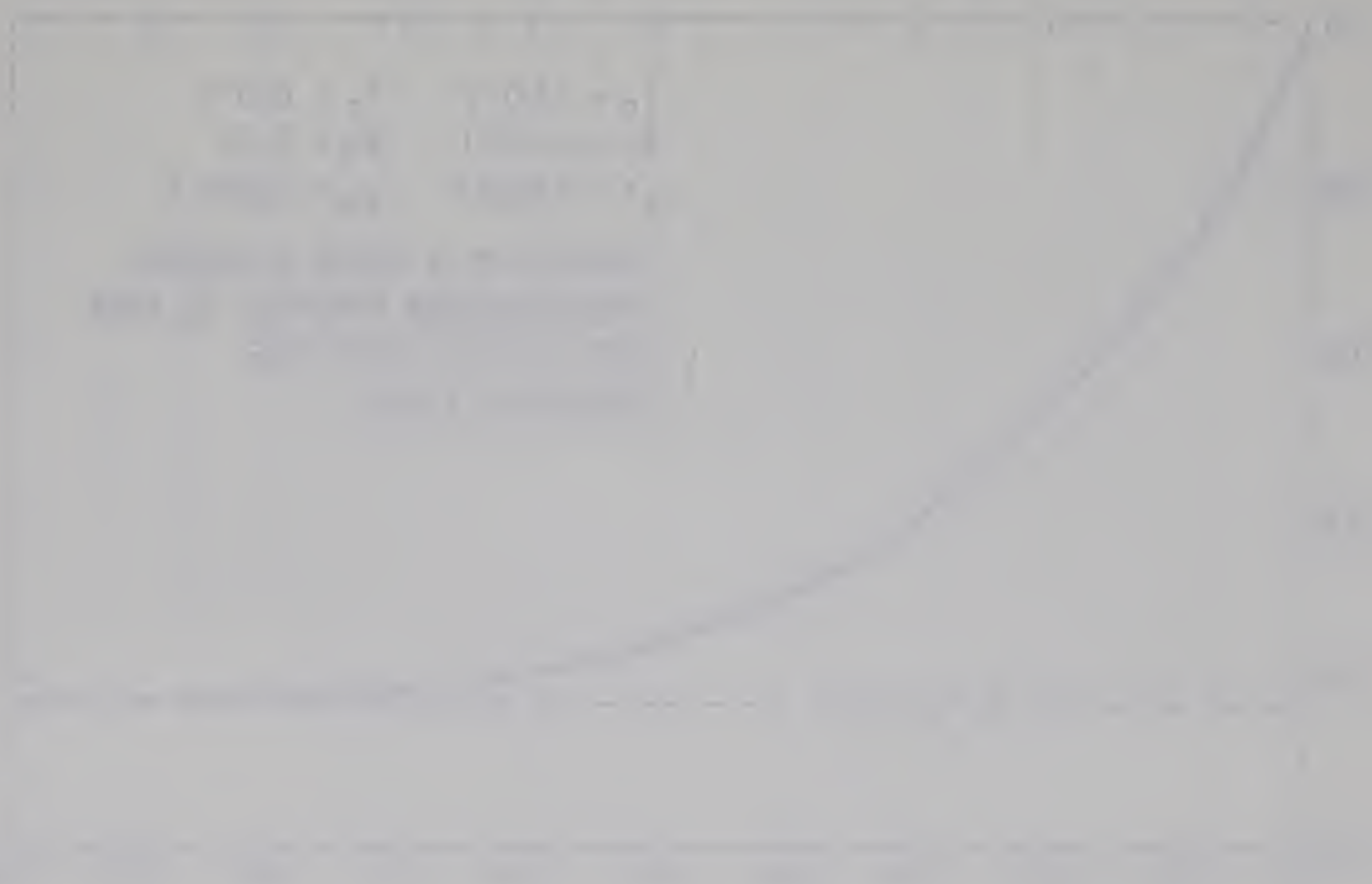

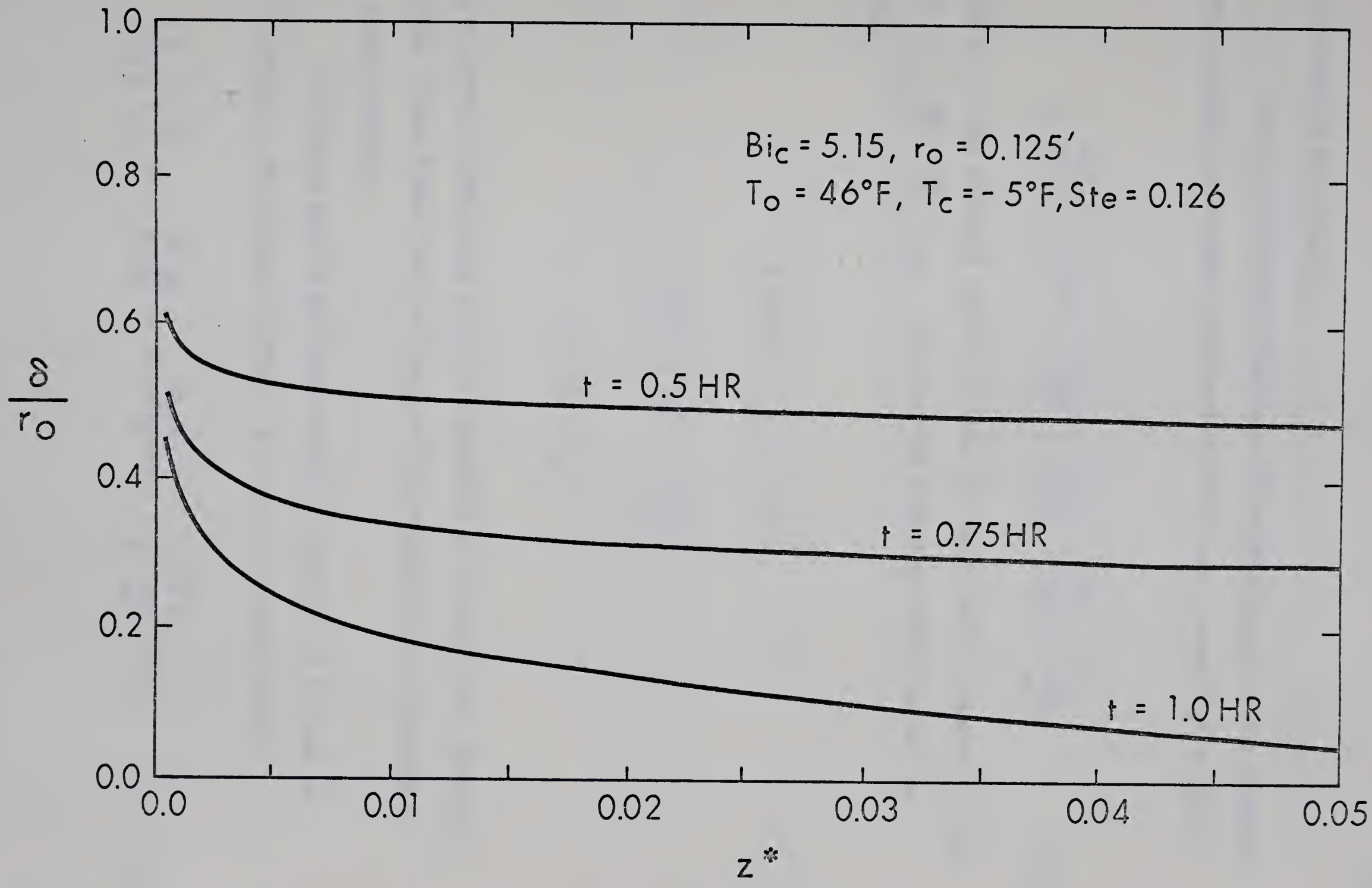

FIGURE 4.2 INTERFACE POSITION VS. LENGTH (FIXED FLOW RATE)

4.2 Pressure Distribution

The axial momentum equation within the liquid in the freezing zone, assuming axi-symmetry and negligible natural convection is given by

$$v_r \frac{\partial v_z}{\partial r} + v_z \frac{\partial v_z}{\partial z} = - \frac{1}{\rho} \frac{\partial p'}{\partial z} + \nu\left[\frac{1}{r} \frac{\partial}{\partial r} \left(r \frac{\partial v_z}{\partial r}\right) + \frac{\partial^2 v_z}{\partial z^2}\right] \qquad 4.2\text{-}1$$

where p' is the pressure departure from the hydrostatic pressure at the wall, i.e. $\frac{\partial p'}{\partial z} = \frac{\partial p}{\partial z} + \rho_w g$. The correct boundary conditions may be stated

$$v_r(\delta,z) = v_z(\delta,z) = 0$$

$$v_z(r,0) = 2V\left[1 - \left(\frac{r}{r_0}\right)^2\right]$$

$$p'(r,0) = p_0' \quad .$$

From an order of magnitude analysis (Appendix B) of the radial momentum equation it was found that the pressure is predominantly a function of the axial position.

Following Zerkle and Sunderland [5], equation 4.2-1 may be multiplied by r and integrated from r = 0 to r = δ, resulting in

$$\frac{d}{dz} \int_0^\delta v_z^2 \, r dr + \frac{\delta^2}{2\rho} \frac{dp'}{dz} = \nu\delta \frac{\partial v_z(\delta,z)}{\partial r} + \nu \int_0^\delta \frac{\partial^2 v_z}{\partial z^2} \, r dr \qquad 4.2\text{-}2$$

using the continuity equation and integration by parts. Substituting the parabolic velocity, v_z, and non-dimensionalizing, the above equation becomes

$$\frac{dp^*}{dz^*} = -\frac{16}{3\delta^{*5}} \frac{d\delta^*}{dz^*} + \frac{32Pr}{\delta^{*4}} \left[1 + \left(\frac{d\delta}{dz}\right)^2\right]$$

where $$p^* = \frac{p_0' - p'}{\rho V^2} .$$

Now if $\left(\frac{d\delta}{dz}\right)^2 << 1$, then upon integration this becomes

$$p^*(z^*) = \frac{4}{3\delta^{*4}} (1 - \delta^{*4}) + 32Pr \int_0^{z^*} \frac{dz^*}{\delta^{*4}} \qquad 4.2\text{-}3$$

The quantity δ^* in this expression is obtained from previous results, i.e. $\delta^* = 1 - r_p \varepsilon$, where ε is calculated for a specific time and tube radius. A representative result is shown graphically in Figure 4.3.

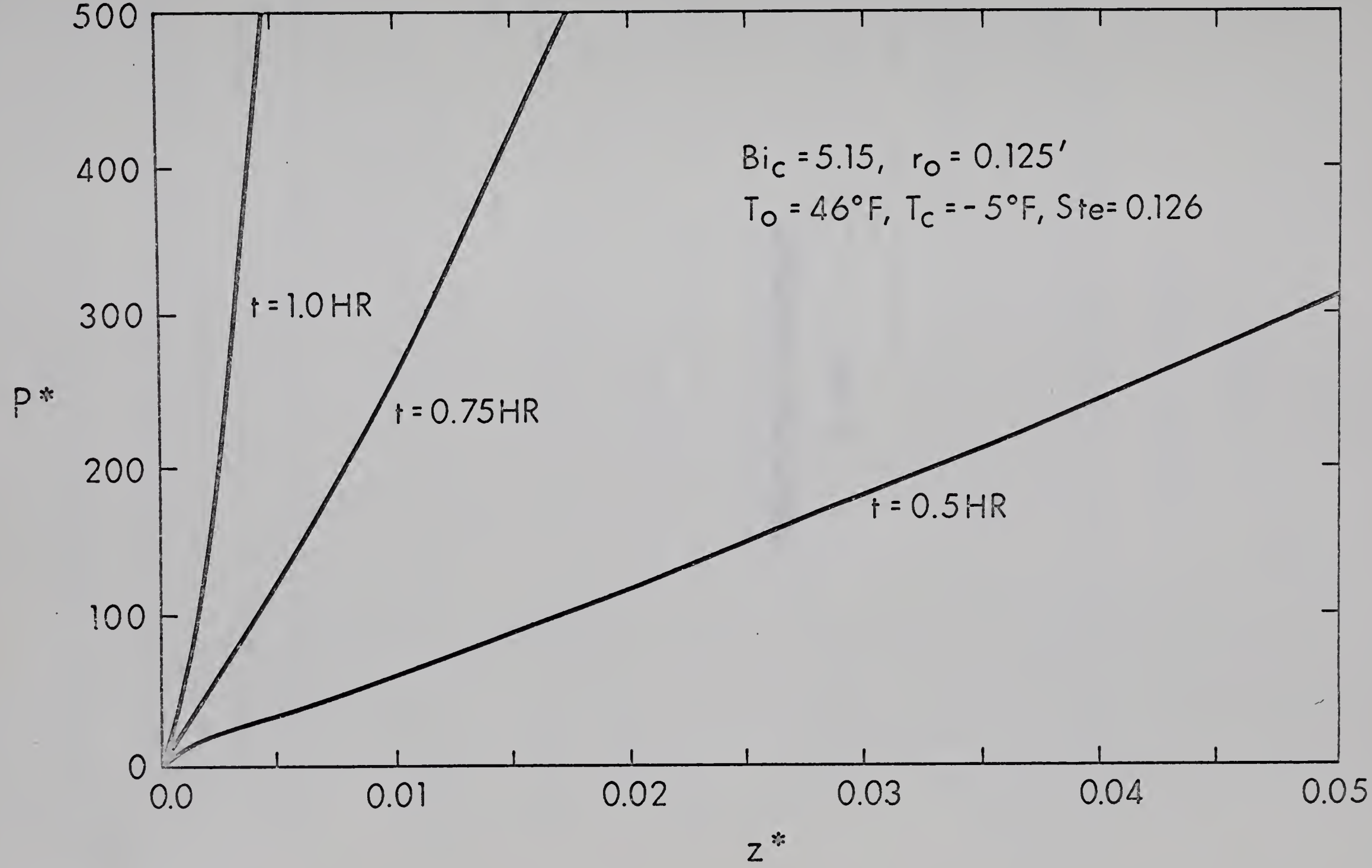

FIGURE 4.3 PRESSURE DROP VS LENGTH (FIXED FLOW RATE)

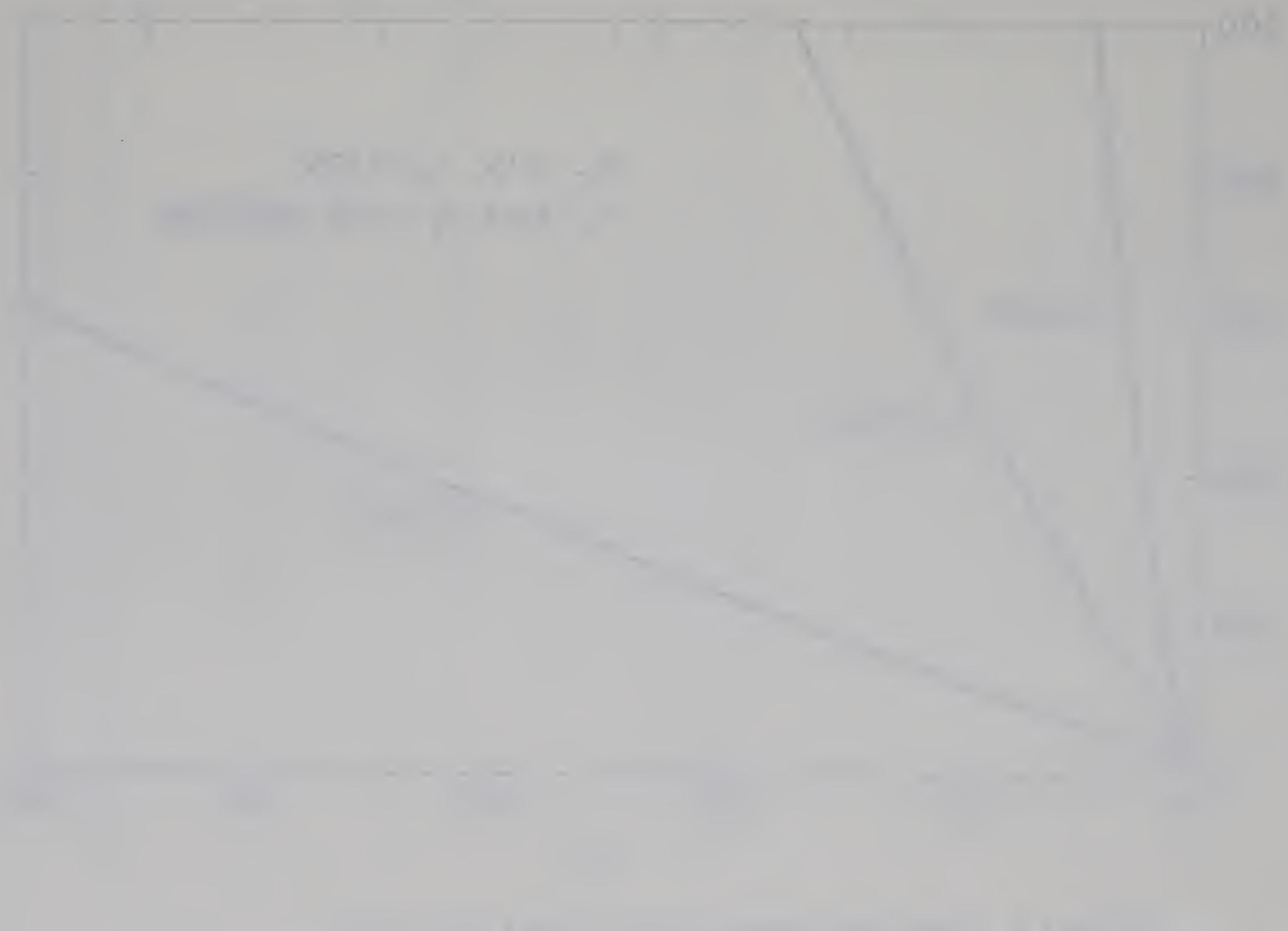

PART II

EXPERIMENTAL INVESTIGATION

11 Jury

CHAPTER V

DESIGN OF APPARATUS

The experimental apparatus was considered as two systems; one for controlling the external boundary condition and the other for the internal fluid flow (see Figure 5.1). The system controlling the external boundary condition consisted primarily of the reservoir and piping for the transport of the cooling agent (a mixture of 50% water and 50% ethylene glycol) to the test section cooling jacket. The coolant was stored in a closed reservoir, 1 - 1/2 feet in diameter and 2 feet high, which contained a cooling coil connected to one of two vapor-compression refrigeration units. This particular unit had a capacity of one ton per hour enabling the coolant to be maintained at a constant temperature of -15°F. The reservoir was connected to the cooling jacket through a one inch diameter copper tubing recirculating system, containing a motorized three-way valve and pump.

A resistance bulb thermometer (L 7033A Balco), which was located about one foot downstream of the three-way valve, was used in conjunction with a resistance thermometer controller (Honeywell R7087D) which controlled the motor (Honeywell M904 Modutrol Motor) linked to the three-way valve (Honeywell Series 1616 three-way valve). The system pump recirculated the coolant from the jacket either into the main reservoir or to the three-way valve which regulated the mixing of the - 15°F coolant

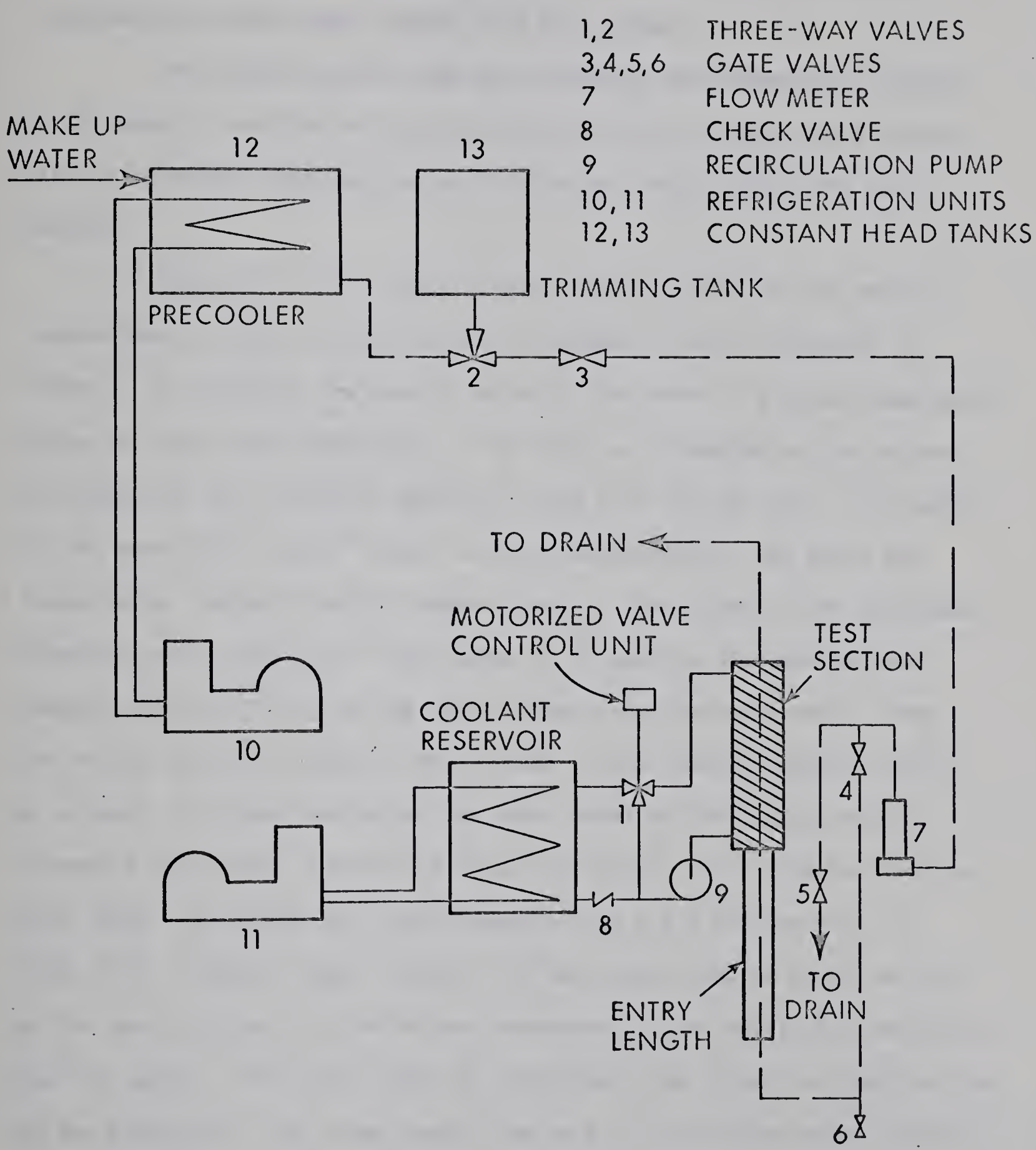

FIGURE 5.1 SCHEMATIC OF EXPERIMENTAL APPARATUS

from the reservoir in order to maintain a constant temperature set on the resistance thermometer controller. The reservoir and piping were insulated to prevent heat leakage into the system.

The second system, used for the supply and temperature control of the water, consisted of two constant head tanks, supply and discharge piping, motorized three-way valve, flow meter, entry length and test section.

The water in the larger header tank is cooled to the desired temperature by a coil around which an ice bank of fixed thickness is formed. The ice bank was used to maintain the water at a given temperature below the water main temperature. The coil was connected to the second refrigeration unit having a capacity of one half ton per hour. The water in the second and smaller header tank was maintained at the water main temperature. Water from both header tanks is then piped to the motorized three-way valve where the "cold" water is trimmed to the appropriate temperature by mixing with the "warm" water from the small tank. From the mixing valve the water is fed through 1 inch diameter copper tubing to a level of eleven feet below the water level in the tanks, passing through a flow meter (Fisher and Porter Ratosight) and a flow controlling gate valve. The water was then channeled into a six foot section of three inch diameter copper tubing, the last three feet of which served as the test section: the latter was surrounded by the previously mentioned cooling jacket. The water could be discharged from either the test section or the flowmeter. The large header tank and all the piping were insulated.

CHAPTER VI

INSTRUMENTATION

The prime instrumentation problem involved the measuring of the ice thickness inside a long vertical pipe surrounded by a completely insulated cooling jacket. Gort [8], met this difficulty with a stainless steel probe with mechanical arms to detect the ice-water interface. A potentially superior method demonstrated by Bailey and Dula [12] employs ultrasonics and it was decided to adopt this approach. The ultrasonic equipment (Branson Instruments Sonoray 600) was operated as a pulse-echo device. A single 1/2 inch cubical immersion transducer facing in a radial direction, attached to a 1/2 inch O.D. stainless steel probe, acted as both transmitter and receiver. The probe was located along the axis of the test section, with the time lag between the echo from the tube wall and the echo from the ice-water interface determining the ice thickness. An analog signal of the ice thickness was obtained through the use of an electronic timing gate (Branson Time Analog Gate): the time lag represented precalibrated ice thickness. The calibration was accomplished using equivalent ice thicknesses in aluminium and then checking and recalibrating the gate using a previously-used apparatus for studying planar ice growth (see Gunderson [13]). An illustration of the pulse-echo signal obtained is shown in Figure 6.1. The accuracy of the instrument is 0.005 inches or better depending on the position of the interface. Since the ice was not isothermal, thus modifying the velocity of sound, there is an

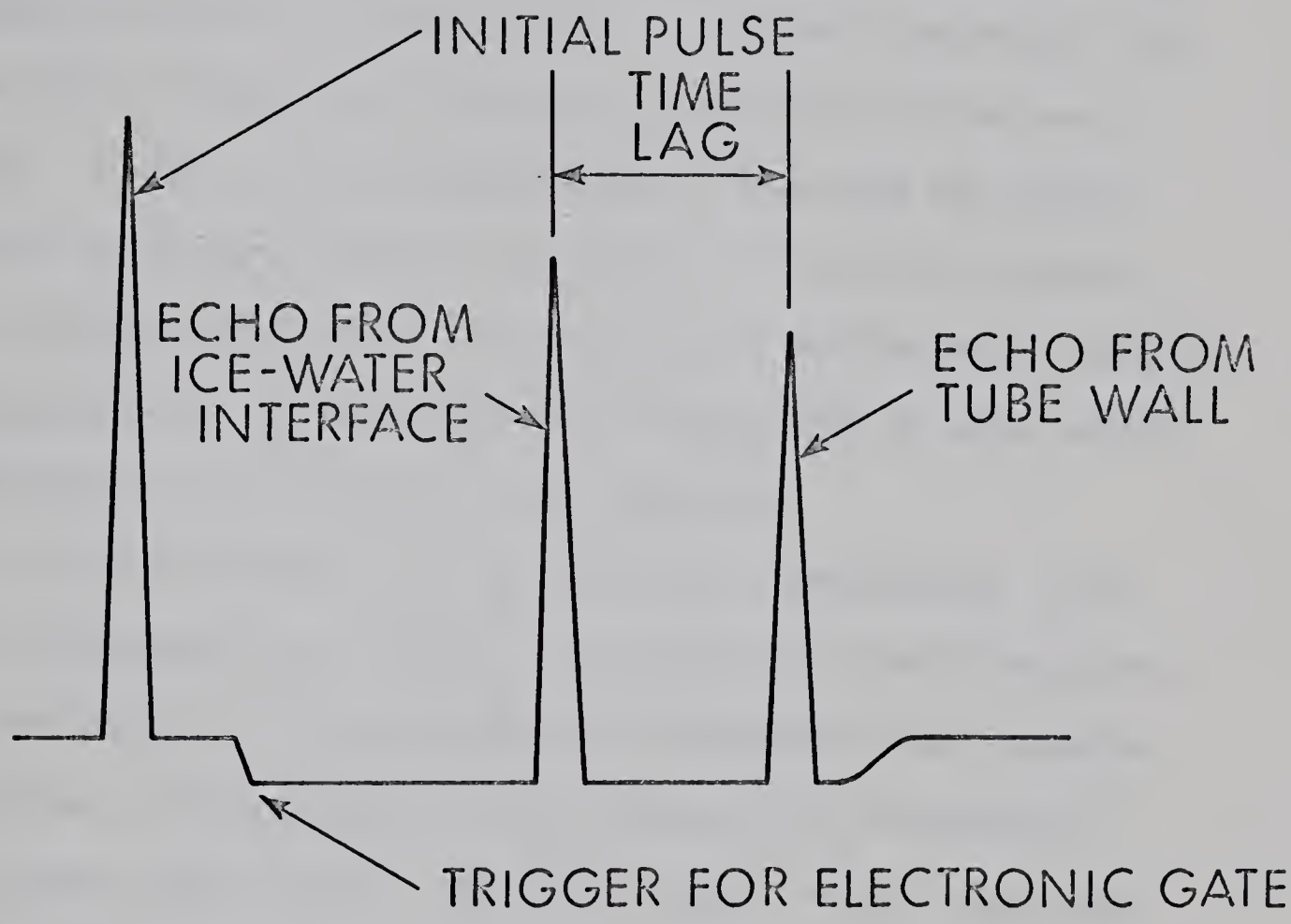

FIGURE 6.1 PULSE - ECHO OPERATION

error inherent in the readings. This error was found to be very small since the temperature gradients were approximately the same during the experimental runs as those during the calibration procedure.

The probe was able to move up and down in the test section by means of a reversing D.C. motor driving a lead screw, to which the one-half inch diameter probe was attached. This position of the probe was then monitored by a forty turn potentiometer: a change in potential from a prescribed datum indicated the distance of the probe from the test section entry. A signal from the potentiometer along with the analog signal from the ultrasonic gate was then used to drive an X-Y recorder, with the ice thickness plotted on the vertical axis and the axial position on the horizontal axis. By this means it was hoped that an axial profile of the ice thickness at any time could be generated.

In order to maintain the desired coolant temperature, a resistance bulb thermometer was located in the coolant recirculating line, as outlined previously. This resistance bulb thermometer was connected to the temperature control mechanism which compared the thermometer's signal to a preset control valve. The error signal, if any, energized the motor controlling the valve movement thus opening the valve for either the - 15°F coolant or the warmer coolant recirculated from the jacket, depending on the polarity of the signal. The three-way valve operation for control of the water temperature was similar, except that an iron-constantine thermocouple sensor was used and the valve movement was controlled manually by the use of a three-way toggle switch.

Further instrumentation consisted of a series of iron-constantine thermocouples, with a resolution of ± 0.25°F, located on the outside wall of the test section at discrete positions and two thermocouples located in the center of the tube six and nine inches before the test section. Readings were obtained during the test period using a low sensitivity sixteen channel recorder (Brown-Honeywell), with a range of - 50°F to + 100°F.

CHAPTER VII

EXPERIMENTS

7.1 No-Flow Tests

A series of tests were conducted without water flowing through the test section in order to determine the reproducibility of the results and make a comparison with theory and other experiments (see Gort [8]).

Before each series of tests the water in the large header tank was cooled over a prolonged period. The test section was then completely drained and the cooling jacket recirculating pump started with the coolant temperature control set at the desired temperature. After waiting to ensure the stabilization of the temperature of the coolant in the cooling jacket,the valve to the test section was held open until water was seen exiting from the discharge line of the test section. The valve was then closed and the time noted. This time was now considered to be the datum, i.e. $t = \tau = 0$. The ultrasonic timing gate was then adjusted carefully along with the gain on the ultrasonic pulse generator so as to trigger on the ice-water interface. Since the analog gate output for one inch of ice was 10^{V}, readings of ice thickness were obtained either from the X-Y recorder or a digital voltmeter. The wall temperatures were then taken at approximately the same time. This procedure was continued until the ice-water interface was within a fifth of an inch of the transducer face. The coolant temperature

control was then set past the freezing point and warm water passed through the test section thus melting the ice. After the ice was completely melted the warm water was shut off and the test section drained. The coolant temperature control was reset to the desired temperature in preparation for the next experiment.

7.2 Laminar Flow Tests

The next series of tests was conducted to determine the influence of flow and superheat on the rate of ice formation and make a comparison with theoretical predictions.

With the coolant temperature control set past the freezing point, the flow was then directed into the test section where its flow was measured and the amount of superheat set using the entry region thermocouples. Once the flow and superheat was established and fixed, the water was then discharged from the flowmeter. Then the procedure for preparing the test section was executed, as in the no-flow tests. The desired temperature of the coolant was set on the controller, the pump started and allowance made for the coolant temperature into the jacket to reach a steady value. With the system in a steady condition, the flow was then switched back to the test section with the datum time noted. Thickness and temperature readings were then taken with the flow being checked periodically by weighing the discharged water over a definite period of time. The end of each test was determined by the prevailing flow and superheat ratios. Each test was terminated when there was no

significant change in ice thickness after fifteen minutes or the ice grew within a fifth of an inch of the transducer face: a test was terminated if the superheat of the water rose substantially making the subsequent results useless for comparison. The test section was then prepared for the next experiment in the same manner as the no-flow tests: coolant temperature control set past the freezing point, warm water used to completely melt the ice, and the test section drained.

PART III

DISCUSSION AND CONCLUDING REMARKS

CHAPTER VIII

DISCUSSION

8.1 No-Flow Problem

This series of experiments was conducted without flow, as discussed previously, to determine the reproducibility of the results and to make a comparison with other experiments and theory. The theory for the no-flow problem in the absence of superheat is essentially the same as for the problem where a liquid is flowing with its bulk mean temperature at the freezing point.

A series of four tests were run, with the water temperature maintained as close to the freezing temperature as possible. The results were compared with those obtained by Gort [8], who assumed the wall temperature difference decreased according to a power law. Using Gort's approach, i.e. a Dirichlet boundary condition, the results obtained for the no-flow tests were in close agreement (see Figure 8.1) and reproducible.

All readings were taken at twenty seven inches from the leading edge of the test section. This was done since the ultrasonic transducer was then opposite two thermocouples which were used to determine a mean heat transfer coefficient at this point. During one of the tests a limited axial traverse of the interface was undertaken using the digital voltmeter: that is, four inches either side of this position. It was found that the profile did not change appreciably (less than 0.008 inches).

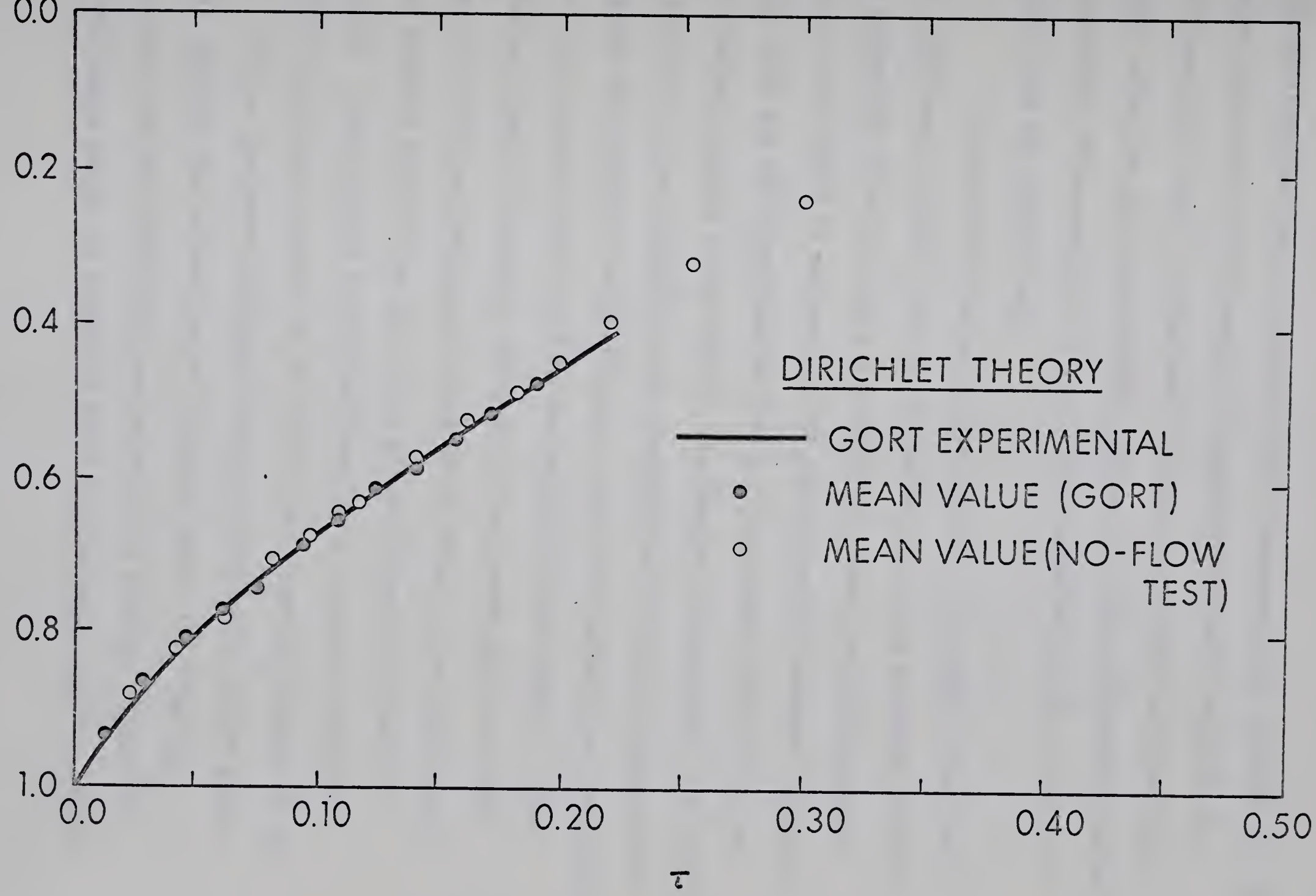

FIGURE 8.1 NO - FLOW RESULTS

This position was then considered to be a representative location for the theory since the rate of growth is independant of axial position for this particular case. A mean heat transfer coefficient was then calculated, using the wall thermocouple readings and the corresponding coolant temperature, from equation 3.3-1.11. This revealed that $\overline{Bi}_c = 5.15$, 27 inches from the leading edge.

The theoretical curve of δ/r_0 versus τ is plotted, along with the experimental results, for the evaluated convective boundary condition. The comparison given in Figure 8.2 shows that there are three possible factors which would be responsible for the discrepancy between the experimental data and the corresponding theory. The primary factor would be the superheat present in the water. The greater the superheat, the greater the deviation to be expected as the superheat must first be removed from the water thus causing the experimental curve to be beneath the theoretical curve. The second factor would be the non-zero Stefan number. Since the Stefan number is non-zero, the rate of ice growth would be slower since it is this non-dimensional group which reflects the significance of the sensible heat of the ice. This effect is small as noted in Chapter 9. Finally there is the consideration of natural convection inherent in the test section due to the initial superheat present in the water. At the ice-water interface cooling is continually taking place thereby lowering the temperature of the water toward the freezing temperature, and thus decreasing the value of its density. Since the water was always below its inversion point (approximately 40°F), a circu-

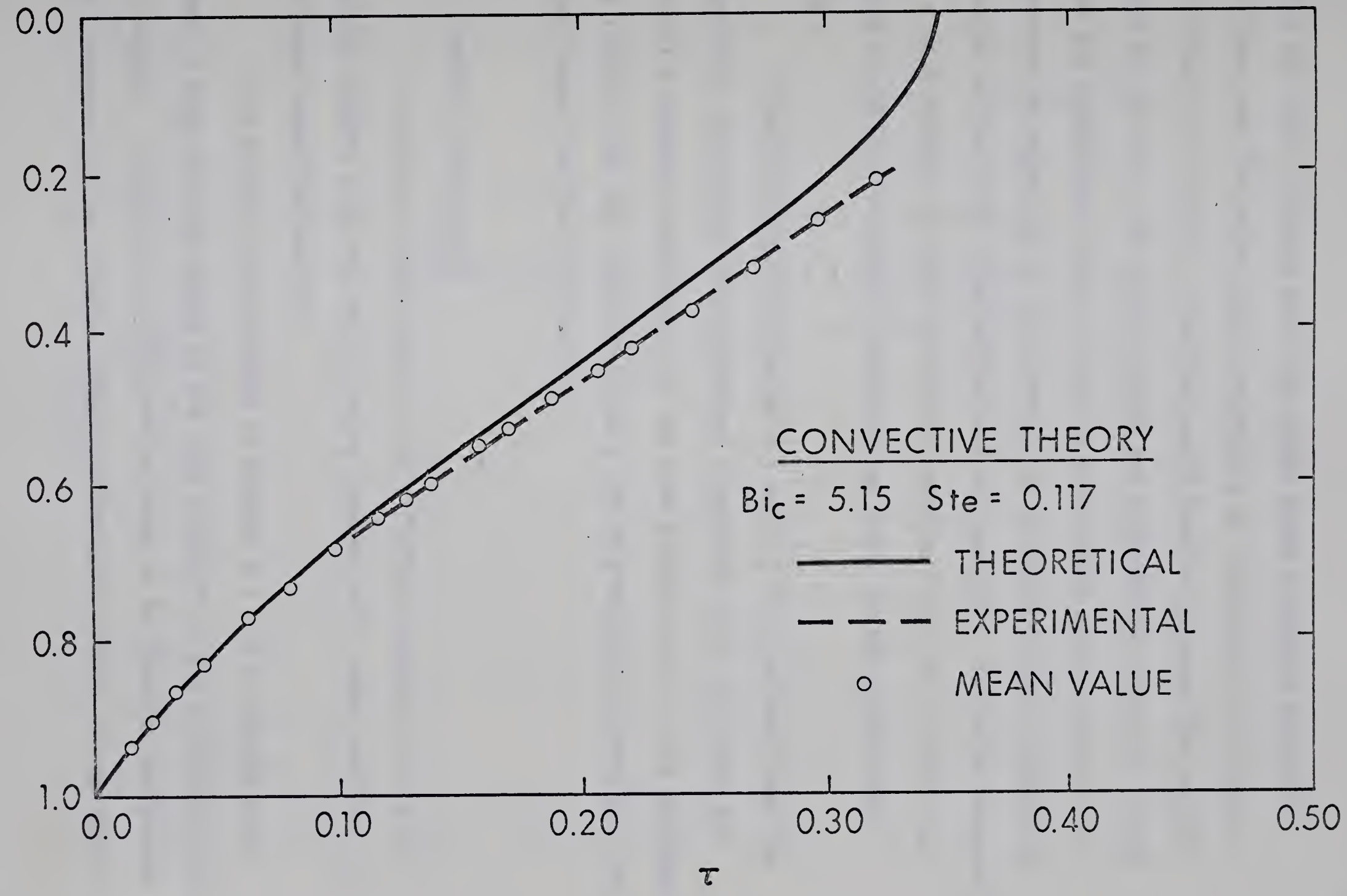

FIGURE 8.2 NO - FLOW RESULTS

lation was then initiated with the colder water ascending along the interface, and the warmer water descending at the center of the pipe. The inclusion of natural convection would tend to decrease the rate of growth of the ice, thus again causing the experimental points to locate below the theoretical curve. Since no experiments were carried out to determine the magnitude of this effect, an estimate of this discrepancy compared to the actual observations was not possible. The water temperature was always brought as close to 32°F as possible (e.g. 34° - 36°F) thus making the effect of natural convection as small as the system would allow.

From superimposing Figures 8.1 and 8.2 it is evident that the theoretical predictions from different viewpoints (i.e. Dirichlet and convective boundary conditions) of the same problem are in close agreement. This reveals that the interface history can be predicted accurately using either theory for the no-flow tests.

8.2 Laminar Flow Problem

A series of tests were run for different superheat ratios and Reynolds numbers with the results being compared with those predicted by the theory developed earlier.

The results are presented in Figures 8.3 - 8.7: the Reynolds number in each test was based on the pipe diameter at the entrance to the test section. Originally, axial profiles were to be taken at designated time intervals during a test. After considerable testing, it was found

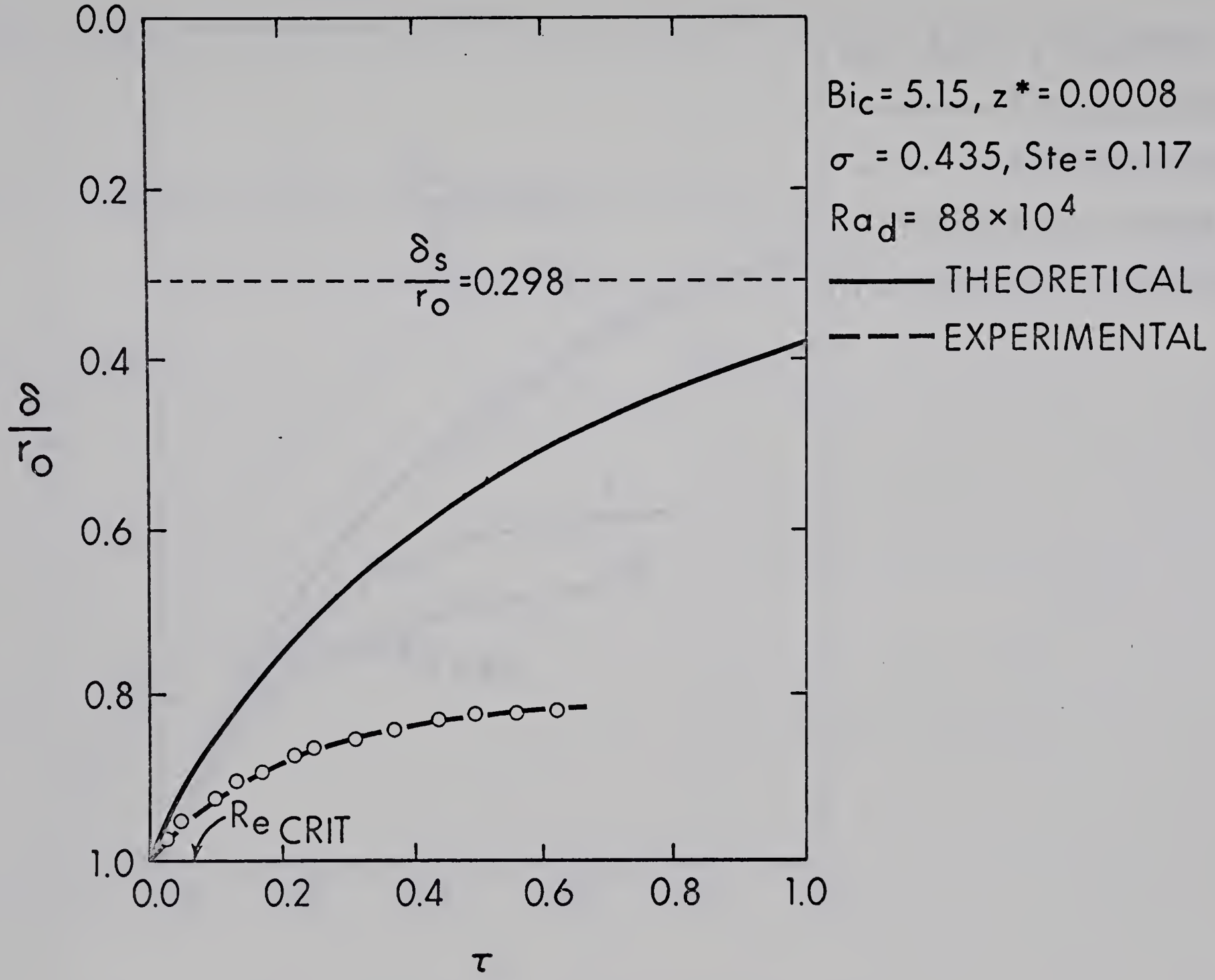

FIGURE 8.3 EXPERIMENT WITH FLOW Re = 2080

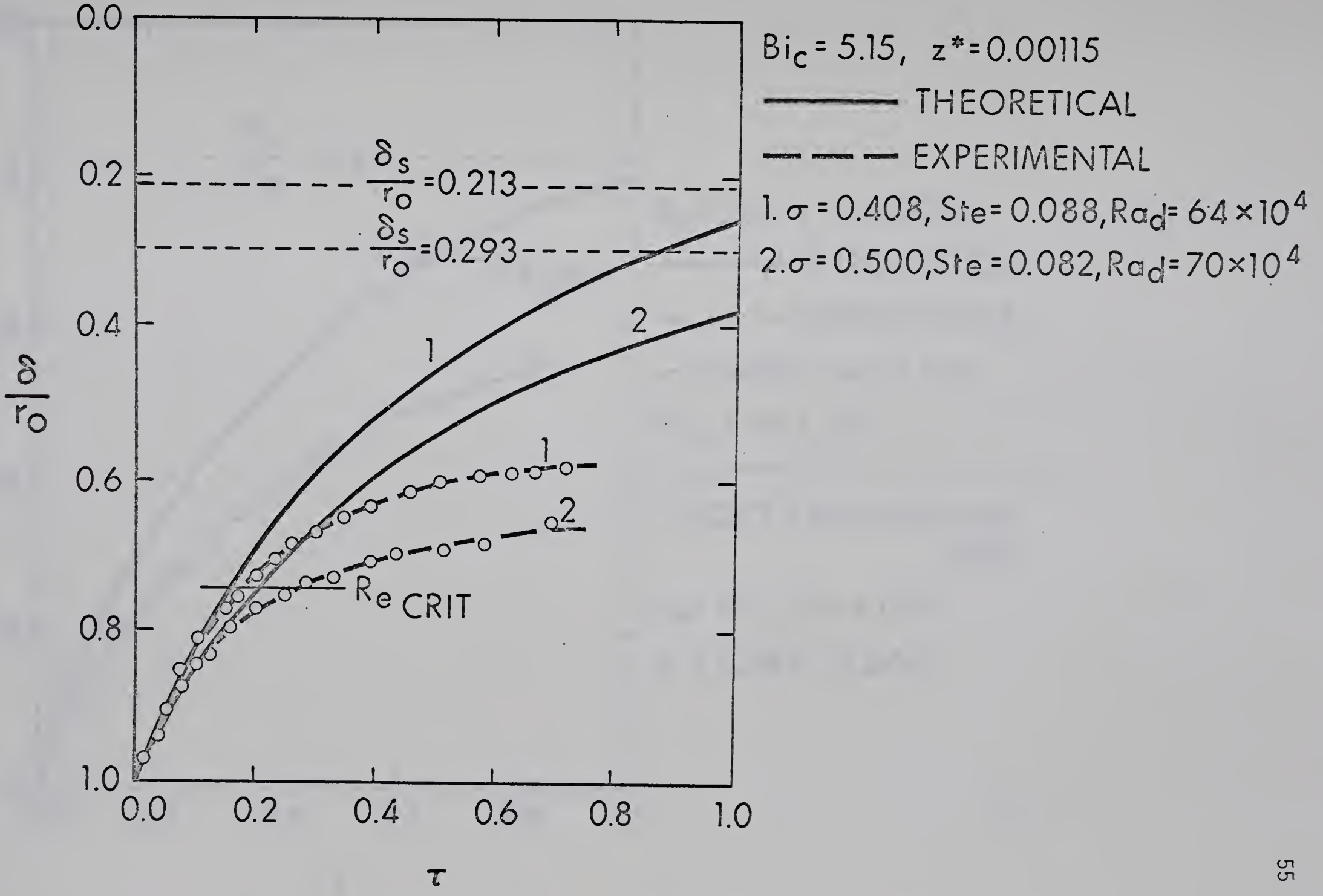

FIGURE 8.4 EXPERIMENTS WITH FLOW Re = 1380

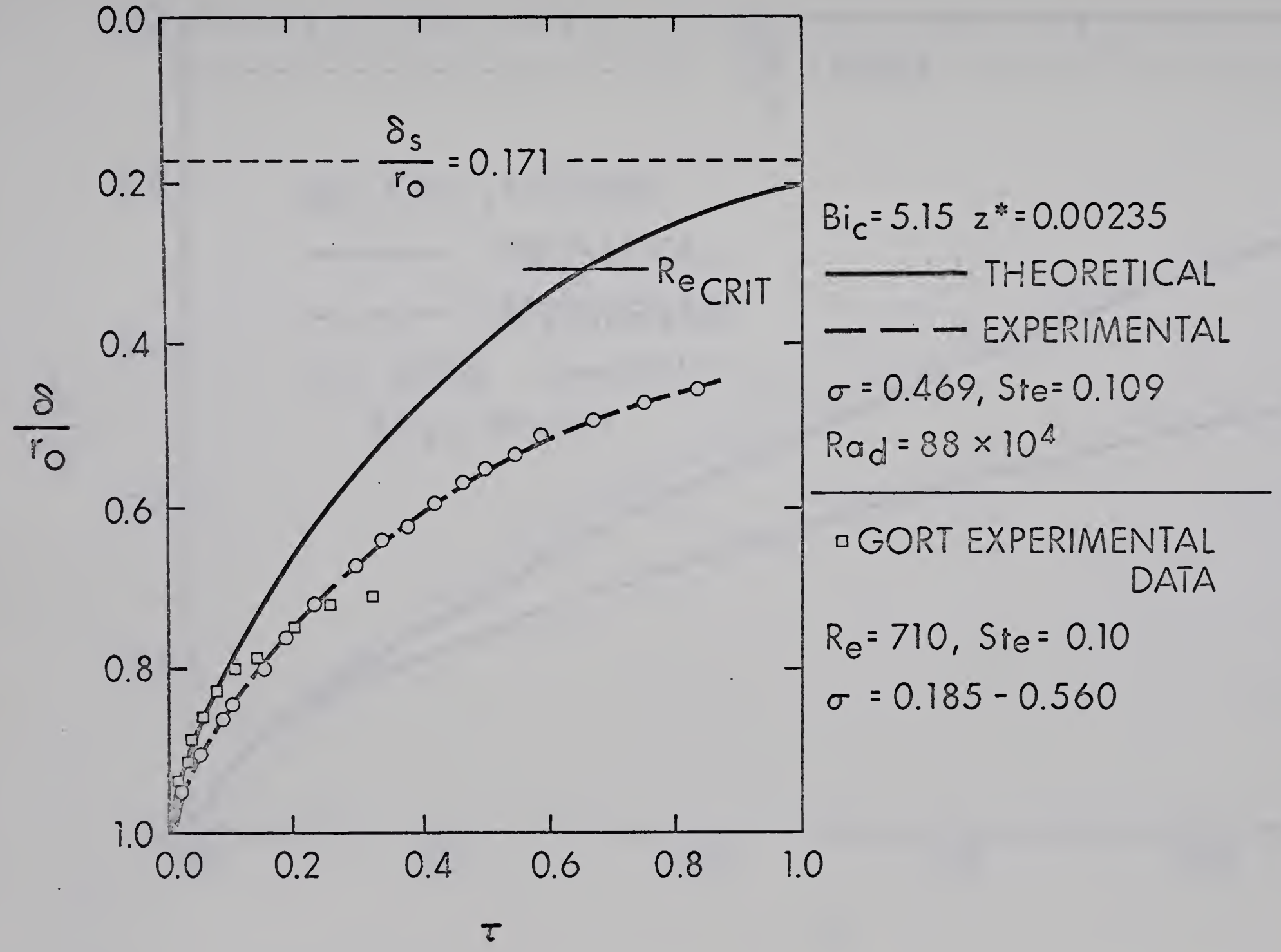

FIGURE 8.5 EXPERIMENT WITH FLOW Re = 690

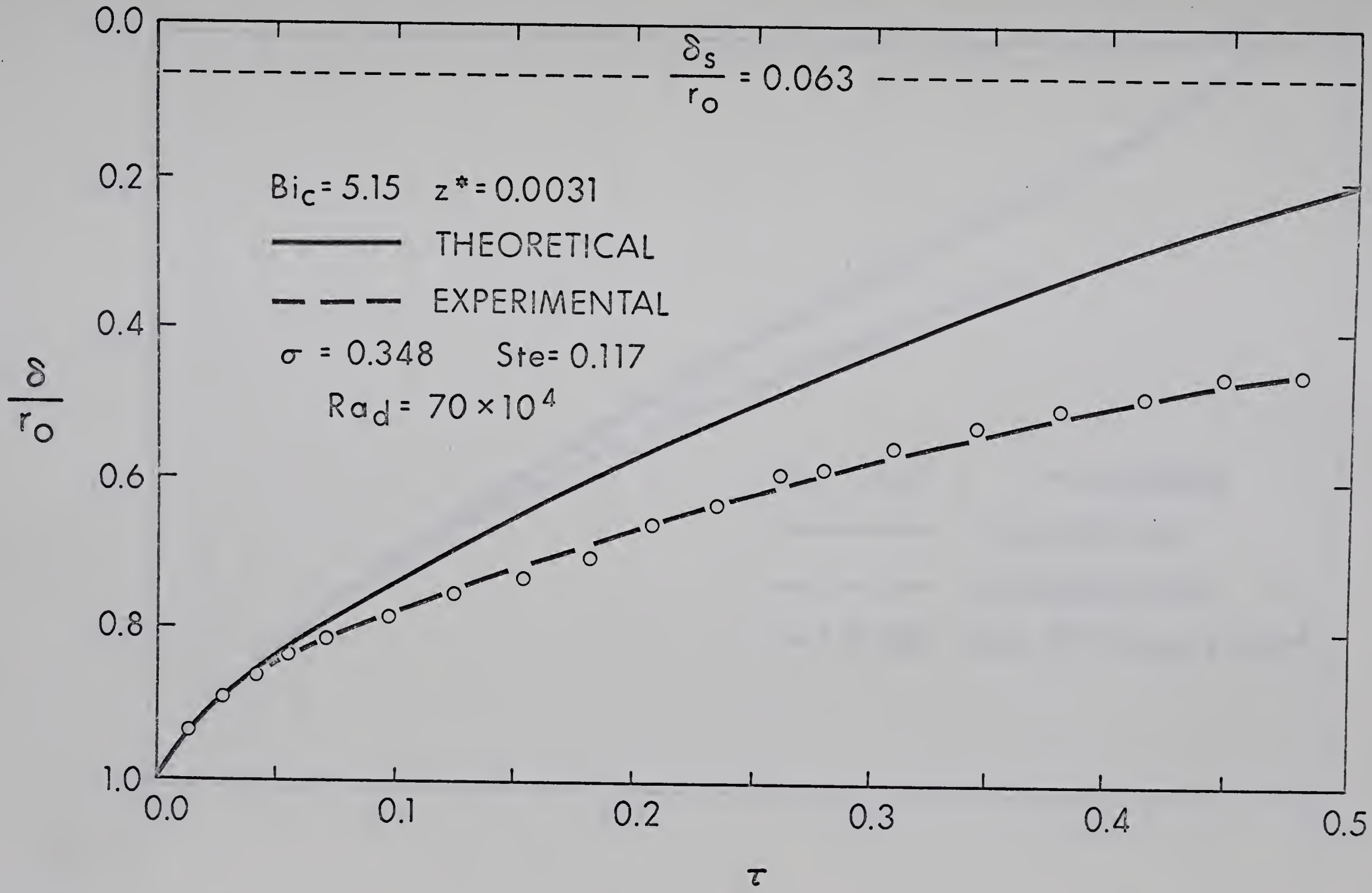

FIGURE 8.6 EXPERIMENT WITH FLOW Re = 518

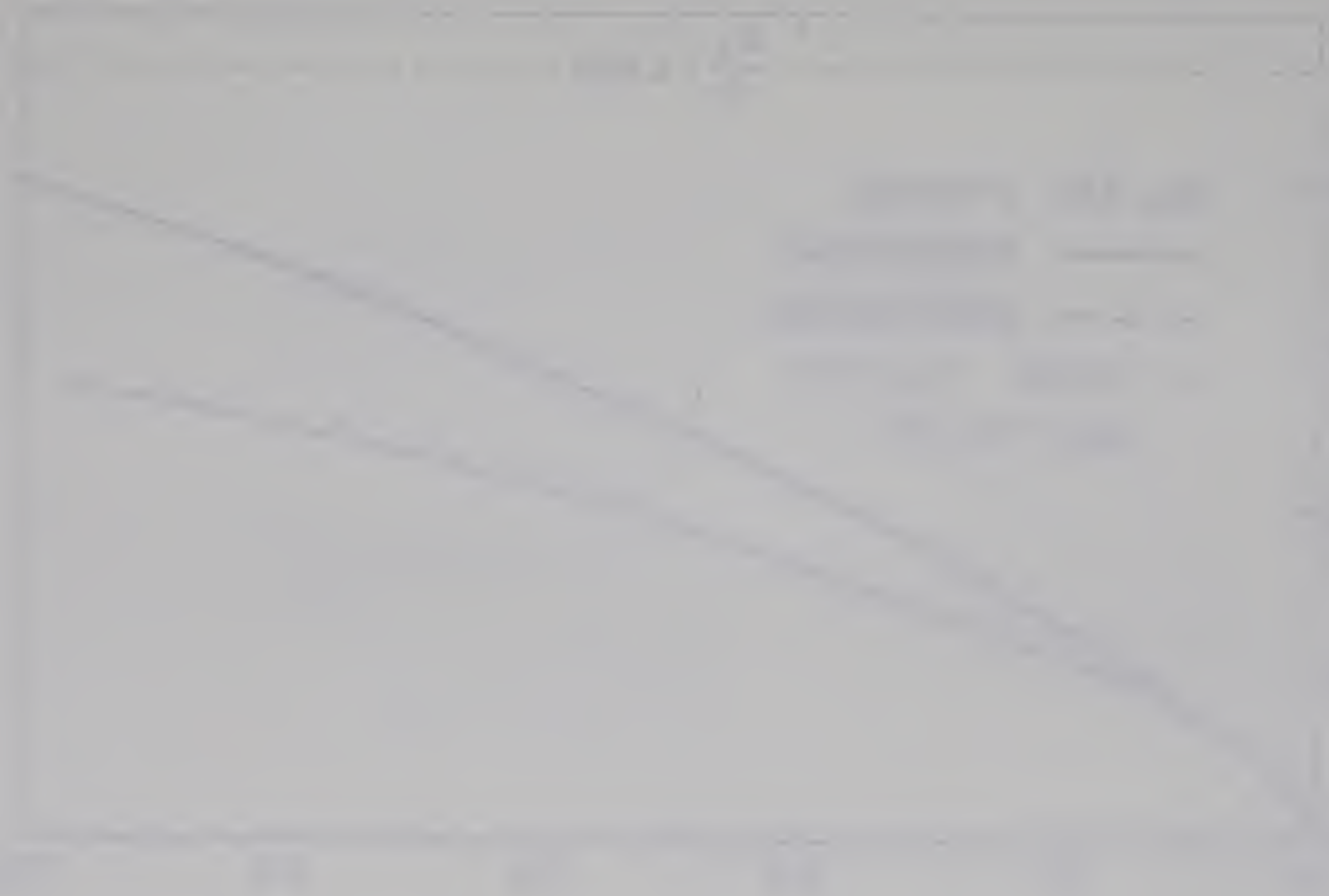

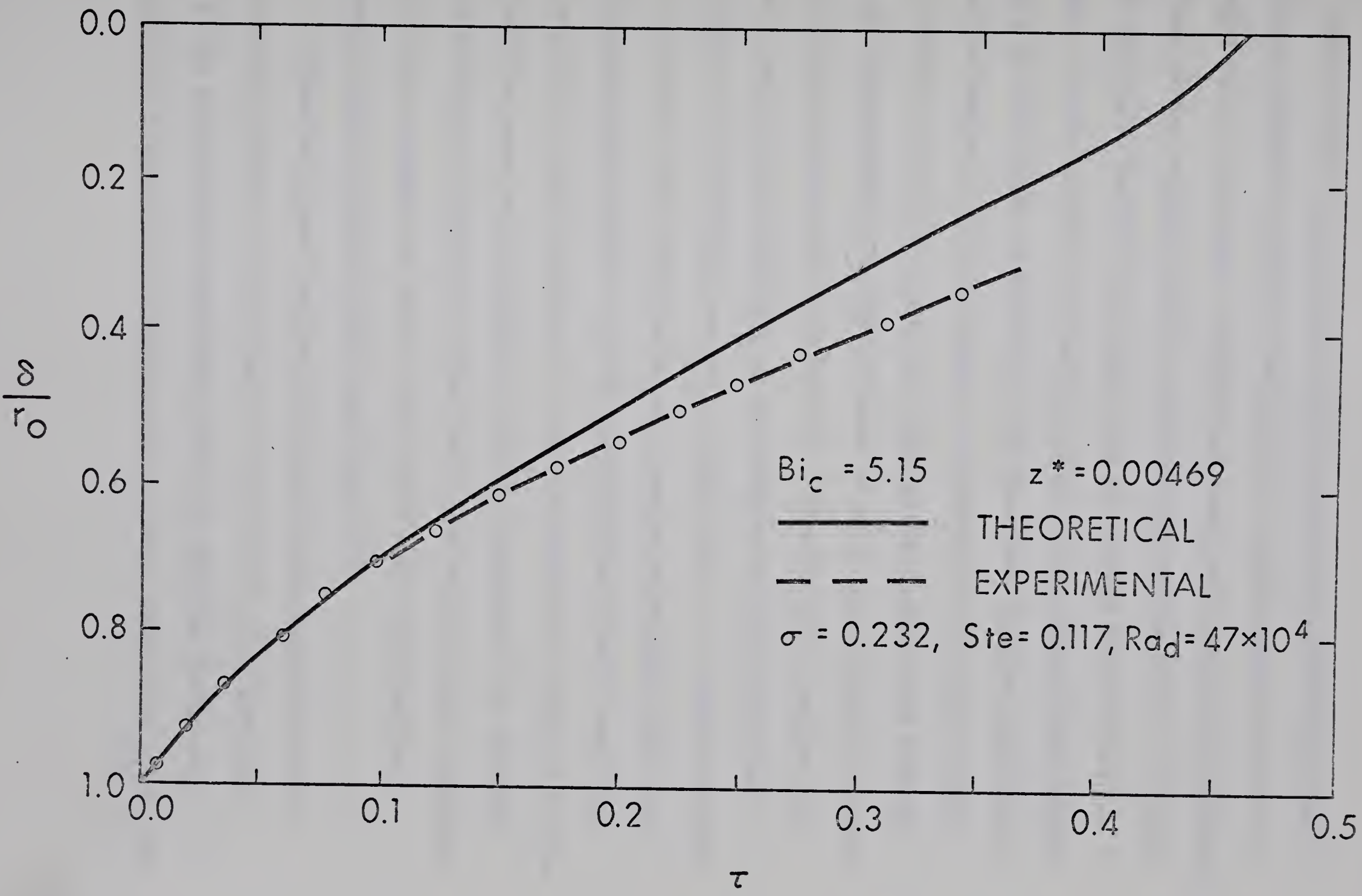

FIGURE 8.7 EXPERIMENT WITH FLOW Re = 345

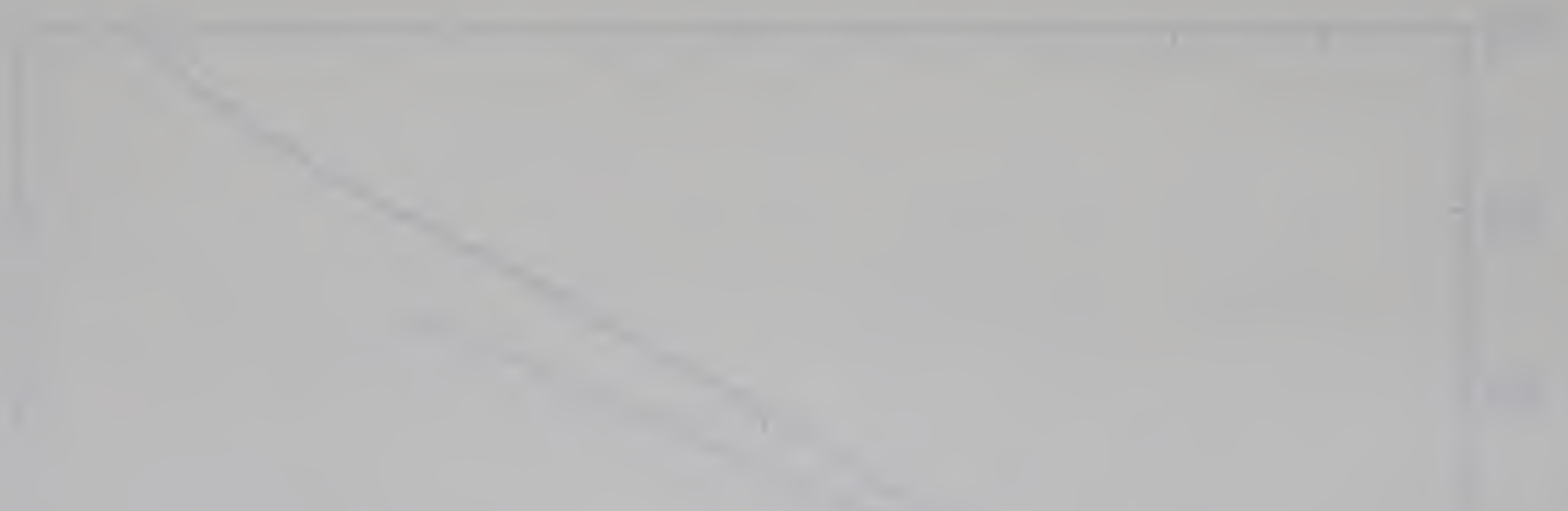

that the ultrasonic equipment was unable to pick up a continuous return of echoes necessary to operate the electronic gate required to obtain a readable plot. The digital voltmeter was then used to obtain the necessary readings at the selected position. As with the no-flow tests, the transducer was placed twenty-seven inches from the leading edge for two reasons. The first one is the desirability of being opposite the thermocouples to facilitate the checking of the mean heat transfer coefficient. The second reason is that the method of discharge of the water from the test section to the drain caused the least disturbance at this location. This was demonstrated by a limited number of axial and azimuthal traverses of the probe done in preliminary testing. The azimuthal traverses also demonstrated that the assumption of axi-symmetry was valid since the variations in ice thickness were only ± 0.008 inches. It should be noted that the ice was still growing when the traverses were made so the variations were probably smaller. During one preliminary test it was found that an ice-free zone did not exist in the test section as expected. Since axial profiles were not obtainable, a check to determine if an ice-free zone existed was not possible. Since the system Nusselt number was large (20.79) it was assumed that an ice-free zone did not exist over the temperature and flow ranges tested (see Figure 2.2).

There are several factors which would explain why the experimental points deviated from the theory. First of all, in Figures 8.3 and 8.4, the flow was high enough that the local Reynolds number was either initially above the critical Reynolds number, taken as $Re_{crit} \simeq 2000$,

or increased, due to increasing ice thickness, to a point where it passed the critical Reynolds number. Since the flow is then no longer laminar, the theory would no longer be applicable beyond this ice thickness. Since turbulent flow results in an increased heat transfer rate, it is reasonable to assume that the steady-state ice thickness would be much lower than that predicted by the laminar flow theory. For these higher flow rates, this increase in local Reynolds number to a point exceeding the critical value would be the dominant factor in the discrepancy between the theory and experiment. The experimental curves of Figure 8.4 are in close agreement with those predicted by theory in that region where the theory is applicable.

Next consider the situation where the initial Reynolds number was low enough to preclude turbulent flow. Here the discrepancies between theory and experiment, shown in Figures 8.5 to 8.7, appears to be a result of the neglect of the effect of natural convection at these lower flow rates. This possibility is supported by an order of magnitude analysis of the momentum equation shown in the Appendix. The circulation now initiated is quite different from that in the no-flow case, as the water temperature is now above the inversion point. The natural convection current alone, without a superimposed forced flow, would then move upward at the interface and at the center of the pipe, though downward in a region between. This effect is quite complicated and it is difficult to say precisely what effect it did have on the flow tests. We know the effect of natural convection will diminish as the water flows through the test section

since its mean temperature approaches the freezing temperature. Therefore the effect of natural convection would be the greatest in the thermal entrance region. This appearance of natural convection causes heat transfer to be greater than theoretical predictions with the result that the radius of the ice-water interface is also greater than the theoretical predictions. Also, as the ice thickness increases along the tube, due to the mean temperature of the water approaching the freezing temperature, the flow area is constricted resulting in the water accelerating and thereby reducing the effect of natural convection in comparison with forced convection. Since no tests were conducted to determine the effect of natural convection it is extremely difficult to say what quantitative discrepancies are involved, except through the order of magnitude analysis.

A comparison was made for one of the flow tests with a similar experimental test made by Gort [8], shown in Figure 8.5. As expected, the data obtained by Gort revealed that the ice grew faster initially and then grew slower as the superheat ratio increased, as opposed to the experimental test run at a constant superheat ratio.

For all set of curves, the question could arise as to whether the experiments were outside the hydrodynamic entry length where the velocity profile is fully developed and the theory applicable. As shown by the theoretical interface profiles at prescribed times, the hydrodynamic entry length increases as the ice thickness increases, i.e. the hydrodynamic entry length is a function of time. This can be demonstrated by Figure 4.2, the position of a particular interface slope, $\frac{d\delta}{dz}$, moves

downstream as the time progressed. If the point at which the experimental results were taken was to be in the entry region, or the entry region increased in time to include this location, then an appreciable error in the theoretical predictions would arise.

For all experimental cases, the effect of the non-zero Stefan number would also have to be considered. This would decrease the rate of growth of the ice due to the inclusion of the sensible heat of the system. The neglect of the unsteady term in the energy equation of the liquid has a very small effect on the theoretical predictions for these experiments, as noted in the Appendix, but would be important for tests involving much larger superheat ratios.

Noting that the average Biot number for the experimental apparatus, at the point considered, was established using results from the no-flow tests. Deviations from the mean value could be expected in some experiments due to the coolant temperature not remaining constant. This would fluctuate the experimental points depending on the temperature variation. Not only will the coolant temperature fluctuate entering the test section but it could vary with axial position. In a counter-flow heat exchanger, as is the experimental test section, the effect would be to increase the coolant temperature as it approaches the leading edge of the test section. This would decrease the predicted steady state radius as well as the complete history of the interface. This effect would be propagated downstream to affect results everywhere. The deviations caused were difficult to assess since axial profiles were unobtainable,

but would likely be noticeable at higher superheat ratios and flow rates. This is possibly substantiated in comparing Figures 8.5 and 8.7.

In the theoretical solution of the ice-free zone, whenever z_e^+ is small, i.e. $z_e^+ < 0.001$, a large number of terms in the series, equation 2.1-10, must be taken. Since the computer program for the ice-free zone did not facilitate a great many terms it was assumed that, for these conditions, $z_e^+ = 0$ and a block temperature profile was then used at inlet to the freezing zone.

For the plane problem Savino and Siegel [7] observed that the experimental transient ice thicknesses were within 15 percent of the theoretically predicted values. The experimental values given here (Figures 8.1 to 8.7) are generally within this departure. Considering the experimental curves overall, it has been demonstrated that the larger the superheat ratio present in the flowing water the more it retards the growth of the ice resulting in a smaller steady state radius. Since the Reynolds number is an indication of the velocity of the water flowing through the test section, it is shown that the increased velocity of the water results in a slower rate of growth due to more superheat per unit time being carried over into the test section. Both these results confirm expectations.

CHAPTER IX

CONCLUDING REMARKS

9.1 Conclusion

This thesis has presented a theoretical and experimental analysis of liquid solidification in a vertical tube, with prescribed convection as the external boundary and interface condition, in the laminar flow regime.

The theoretical approach considered only the asymptotic solution for the temperature profile in the growing ice phase since for ice-water systems the Stefan number is usually much less than unity. The use of this temperature profile in the interface equation yielded an asymptotic solution for the history of the interface. The effect of neglecting the sensible heat effects in the ice, has been shown by Lock [11] to be small for the plane problem. Using the experimental Stefan numbers and superheat ratios from the cylindrical tests, it is not unreasonable to expect that approximately the same error would be introduced in the cylindrical system, at least during the early stages of ice formation when the forming phase would be nearly planar.

The statement of overall heat balance at the interface was found to be dependent upon two dimensionless groups contained in the variable β: the superheat ratio σ, and the conductivity ratio $\frac{k_\ell}{k_i}$. For a given liquid (i.e. k_ℓ and k_i known), the greater the value of σ, the

greater the rate of freezing and thicker is the ice at a given axial position z.

The majority of the theoretical predictions were well borne out by the experimental results obtained within a region where the theory was applicable. A comparison of theoretical and experimental results of $\frac{\delta}{r_0}$ versus τ, for all experiments, generally revealed agreement to within 20% or better. Discrepancies, although never large, were greatest as the ice-water interface approached the center of the tube. On occasions, the signals received by the ultrasonic transducer became random to a degree, e.g. ± 0.020 inches, probably due to the increasing concavity of the interface resulting in the reception of multiple echoes. As mentioned previously the effect of natural convection, as well as the effect of being in the hydrodynamic entry region where the inertia terms are of importance, would have affected the results.

A considerable amount of work was done on the experimental apparatus to try to obtain axial profiles which are quite important in making a complete discussion of the theory and experiment. The various modifications to the apparatus did produce (or lead to) limited axial profiles using the X-Y plotter. A curve is shown in Figure 9.1 with the results unplottable at a distance of 24 inches from the leading edge, as the illustration shows.

9.2 Suggestions for Further Work

The analysis is limited to the history and profile of the ice growth in a vertical tube neglecting natural convection, inertia terms

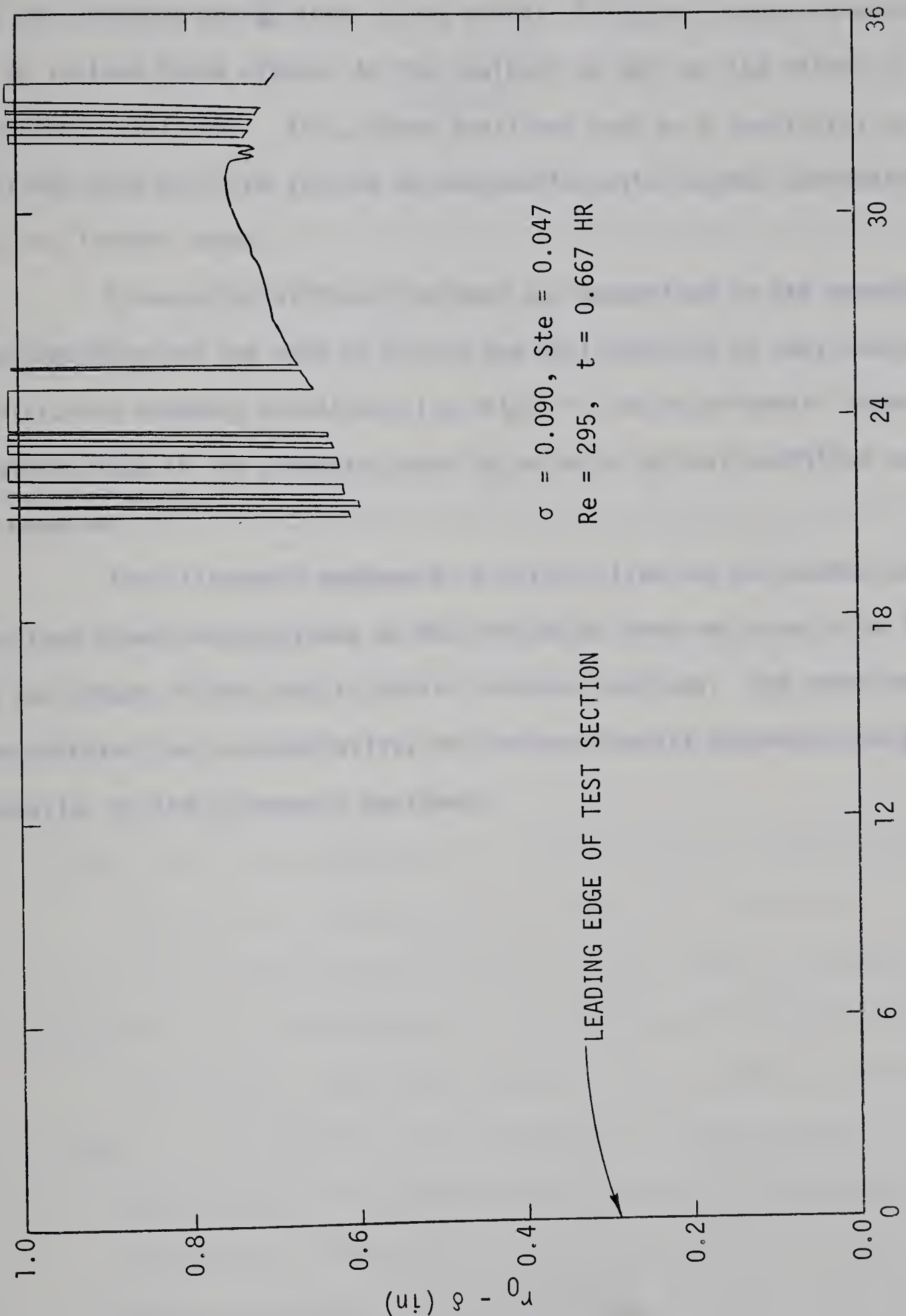

FIGURE 9.1 AXIAL PROFILE TRIAL

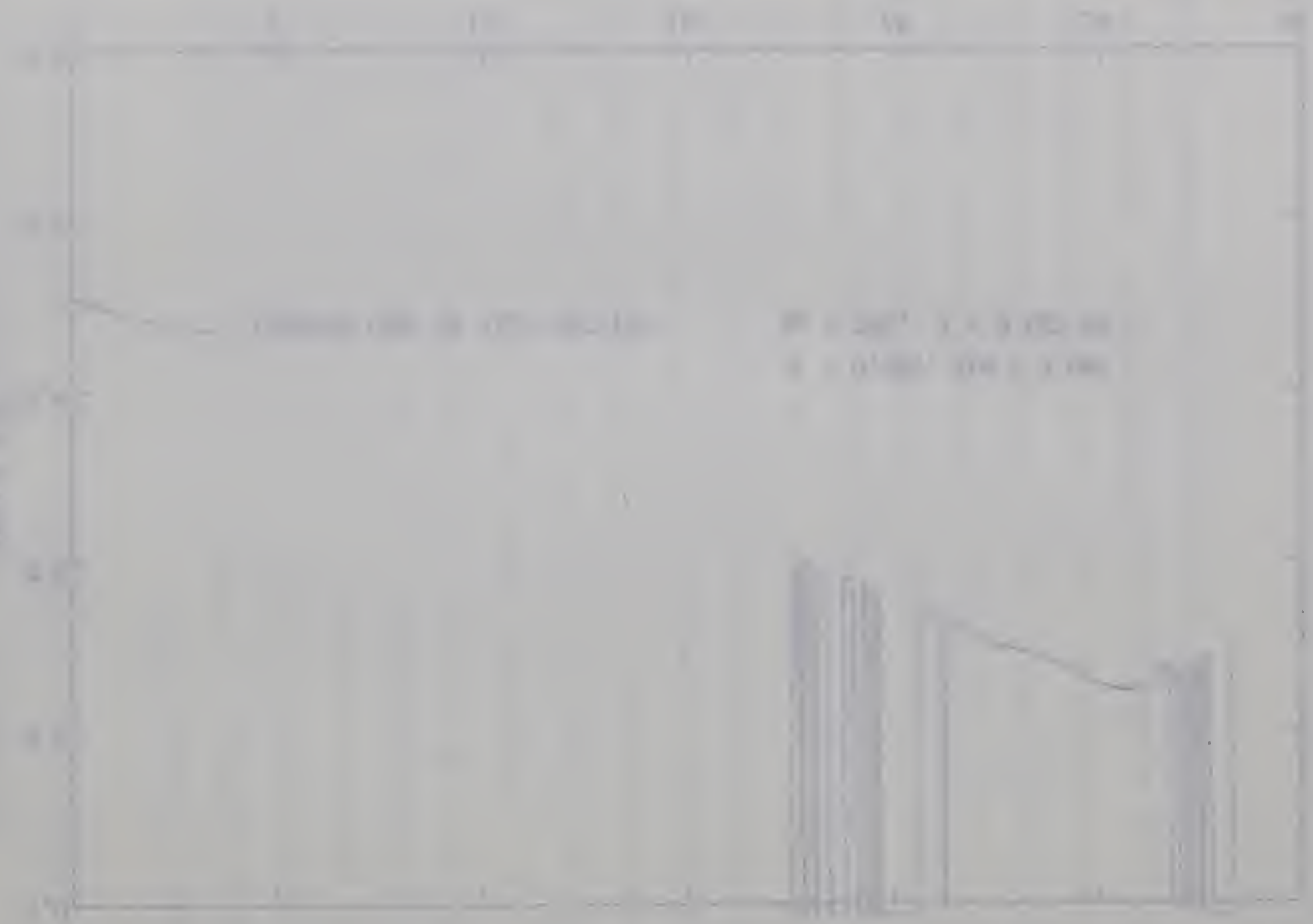

and the unsteady energy term in the fluid. A logical extension would be to include these effects in the analysis as well as the effect of turbulent conditions. Also, other positions such as a horizontal or an inclined tube could be studied in conjunction with natural convection and the inertia terms.

It was also difficult to make any comparison in the experiments reported here and the work of Özisik and Mulligan [14] as they considered a Dirichlet boundary condition, i.e. $Bi_c \to \infty$. An experimental comparison could be made if the apparatus were to be built so this condition could be examined.

The ultrasonic equipment is quite suited for horizontal and inclined tube investigations as the transducer does not have to be located in the center of the tube to obtain accurate readings. The experiments demonstrated the reproducibility of the experimental apparatus and the potential of the ultrasonic equipment.

REFERENCES

1. BRUSH, W.W., "Freezing of Water in Subaqueous Mains Laid in Salt Water and in Mains and Services Laid on Land", Journal of the American Water Works Association, Vol. 3, 1916, pp. 962-980.
2. LONDON, A.L. and SEBAN, R.A., "Rate of Ice Formation", Trans. A.S.M.E., Vol. 65, 1943, pp. 771-778.
3. KREITH, F., and ROMIE, F., "A Study of the Thermal Diffusion Equation with Boundary Conditions Corresponding to Solidification or Melting of Materials Initially at the Fusion Temperature", Phys. Soc. Proc., Sect. B, Vol. 68, Pt. 5, May 1955, pp. 277-291.
4. STEPHENSON, D.G., "Preventing Exposed Water Pipes from Freezing", Unpublished.
5. ZERKLE, R.D., and SUNDERLAND, J.E., "The Effect of Liquid Solidification in a Tube Upon Laminar-Flow Heat Transfer and Pressure Drop", J.H. Transfer, Vol. 90, 1968, pp. 183-190.
6. BEAUBOUEF, R.T., and CHAPMAN, A.J., "Freezing of Fluids in Forced Flow", Int. J. Heat Mass Transfer, Vol. 10, 1967, pp. 1581-1587.
7. SIEGEL, R., and SAVINO, J.M., "An Analysis of the Transient Solidification of a Flowing Warm Liquid on a Convectively Cooled Wall", Proceedings of the Fluid International Heat Transfer Conference, Chicago, A.S.M.E., A.I.Ch.E., Aug. 1966, Vol. IV, pp. 141-151.

8. GORT, C., "Preliminary Study of Ice Formation in a Vertical Pipe", M.Sc. Thesis, University of Alberta, Edmonton, Alberta, June 1968.

9. DesRUISSEAUX, N., and ZERKLE, R.D., "Freezing of Hydraulic Systems", Paper presented at the A.I.Ch.E.-A.S.M.E. Heat Transfer Conference and Exhibit, Philadelphia, Pa., August 11-14, 1968.

10. SELLARS, J.R., TRIBUS, M., and KLEIN, J.S., "Heat Transfer in Laminar Flow in a Round Tube or Flat Conduit - the Graetz Problem Extended", Trans. A.S.M.E., Vol. 78, Feb. 1956, pp. 441-448.

11. LOCK, G.S.H., "On the Use of Asymptotic Solutions to Plane Ice-Water Problems", J. Glaciology, 1969 (in press).

12. BAILEY, J.A., and DULA, A., "Acoustic Technique for Use in Some Solidification Rate Studies", The Review of Sci. Instruments, Vol. 38, No. 4, April 1967, pp. 535-538.

13. GUNDERSON, J.R., "A Study of Heat Conduction with Phase Change", M.Sc. Thesis, University of Alberta, Edmonton, Alberta, 1966.

14. ÖZISIK, M.N., and MULLIGAN, J.C., "Transient Freezing of Liquids in Forced Flow Inside Circular Tubes", presented at A.S.M.E. Winter Annual Meeting, December 1-5, 1968. Paper No. 68-WA/HT-7.

15. HILDEBRAND, F.B., "Advanced Calculus for Applications", pp. 206-213. Prentice-Hall, Inc., 1962.

APPENDIX A

FORTRAN IV PROGRAM FOR THE MERGED PROBLEM

A '*' IN COL. 6 INDICATES THAT THIS
LINE IS A PART OF THE PREVIOUS CARD

```
C
C              CYLINDRICAL  ICE  FORMATION
C
C                   ------
C
C
C              ICE FREE ZONE
C
      DIMENSION XX(4),TP(101,4),DELT(101),R(101,4),T(101),C(
     *  40)
      DIMENSION X(102),Y(102),W(102)
      REAL DATA(1024)
      COMMON BIOT,TF,TC,TL,CICE,CH2O,BI
      COMMON RLAM(40),RLAMW(40),CH(40),CC(40),CK(40),RLR(100
     *  1)
      COMMON RTR(101,40),PRES(101),VA(101)
      COMMON CLI,RHOI,RO
      F(A)=(1.0/BIOT)+((CONST*SIN((A*PI/4.0)-(2.0*PI/3.0)))/
     *  (SIN((A*PI/4
     1.0)-(PI/3.0))*(A**0.666667))
      FF(B)=(1.0/BIOT)+((CONST*SIN((B*PI/4.0)-(2.0*PI/3.0)))
     *  /(SIN((B*PI/
     24.0)-(PI/3.0))*(B**0.666667))
      READ(5,105) TF,TC,TL,Z,BI
C
C              NOTE  ---  BI = RO*HO/K-ICE
C
      READ(5,102) PR,PHO,PMU,CICE,CH2O,CLI,RHOI,RO
      READ(5,700) TIME,MT,MZ,MR
      READ(5,900) IPR,NN,C5,D5,TOR,BOT,DELX,XAX,YAX
      READ(5,101) KONST
C
C              FINDING EIGENVALUES
```

```
C
      PI=3.1415926
      BIOT=BI*CICE/CH20
      CONST=((3.0**0.666667)*GAMMA(1.333333))/((2.0**0.33333
     *  33)*GAMMA(0.
     2666667))
      I=0
      DELW=0.01
      WRITE(6,106)
      WRITE(6,511)
      WRITE(6,508)
      WRITE(6,509) BIOT
      WRITE(6,510) TL
      WRITE(6,500)
C
C              CALCULATE INITIAL GUESS FOR ROOT
C
      A=DELW
   21 B=A+DELW
      SUM3=ABS(F(A)+FF(B))
      SUM4=ABS(F(A)-FF(B))
      IF(SUM4.GT.10.0) GO TO 22
      IF(SUM3-SUM4) 20,20,22
   22 A=A+DELW
      GO TO 21
C
C              FOR DETERMINING ROOT TO THE DESIRED ACCURACY
C              SUBSTITUTE INITIAL GUESS INTO NEWTON-RAPHSON
C              TECHNIQUE
C
   20 A1=A
      B1=B
      ROOT=A1
      ITERNS=30
      ACCRCY=1.0E-6
      CALL TRANS1(ROOT,ACCRCY,ITERNS)
      WRITE(6,501) I,ROOT
      I=I+1
      RLAMW(I)=ROOT
      IF(I.EQ.40) GO TO 23
      A=B1
      GO TO 21
   23 WRITE(6,506)
      WRITE(6,504)
      DO 24 I=1,40
      ROOT=RLAMW(I)
      CALL RLN(ROOT)
      DO 40 JJ=1,101
      JK=JJ-1
   40 PTR(JJ,I)=RLR(JK*10+1)
C
C              CALCULATE COEFFICIENTS ' C  '
C                                      K
```

```
C
      CALL INTEG1(0.0,1.0,SS1)
      CALL NUMER4(0.0,1.0,SS4)
      CK(I)=SS4/SS1
      II=I-1
   24 WRITE(6,501) II,CK(I)
C
C              CALCULATE POSITION AT WHICH THE WALL
C              TEMPERATURE IS EQUAL TO THE LIQUID
C              FREEZING TEMPERATURE
C
      IF(TL.EQ.TF) GO TO 33
      GO TO 34
   33 ZCRIT=0.0
      GO TO 32
   34 CONTINUE
      PHI=(TF-TC)/(TL-TC)
      ERR1=1.0E20
      DO 30 JJ=1,1000000
      ZCRIT=FLOAT(JJ)*0.000001
      SS=0.0
      DO 31 KK=1,40
      RLAW=RLAMW(KK)
      ERP=RLAW*RLAW*ZCRIT
      IF(ERP.GE.174.673) GO TO 50
      GO TO 51
   50 C(KK)=0.0
      GO TO 56
   51 C(KK)=CK(KK)*RTR(101,KK)*EXP(-ERP)
      BAD=ABS(C(KK))
      IF(BAD.LT.1.0E-20) GO TO 57
   56 SS=SS+C(KK)
   31 CONTINUE
   57 ASS=ABS(SS)
      ERR=ABS(ASS-PHI)
      IF(ERR.GE.ERR1) GO TO 32
   30 ERR1=ERR
   32 WRITE(6,106)
      IF(ZCRIT.LT.1.0E-3) GO TO 80
      WRITE(6,600) ZCRIT
C
C              CHECK WALL TEMPERATURE
C
      TFREEZ=(TL-TC)*SS+TC
      WRITE(6,507) TFREEZ
      GO TO 81
   80 WRITE(6,100) TL
C
C              DETERMINE TEMPERATURE PROFILE AT THE INLET
C              TO THE ICE PROBLEM
C
   81 CALL VALUE(ZCRIT)
C
```

```
C                PLOT TEMPERATURE PROFILE
C
      WRITE(6,106)
      WRITE(6,901)
      CALL SKETCH(DELX,IPR,C5,D5,BOT,TOP,NN,XAX,YAX)
      WRITE(6,902)
C
C                CONSIDERING FREEZING ZONE
C
      WRITE(6,405)
      DO 75 K=1,40
      RLAM(K)=(4.0*FLOAT(K-1))+(8.0/3.0)
      RLAMD=PLAM(K)
      CALL PIN(RLAMD)
C
C                CALCULATE COEFFICIENTS ' C   '
C                                        N
C
      CALL INTEG1(0.0,1.0,SS1)
      CALL INTEG2(0.0,1.0,SS2)
      CC(K)=SS2/SS1
      CH(K)=-(CC(K)/2.0)*RLNP(RLAMD,K)
      KK=K-1
   75 WRITE(6,403) KK,RLAM(K),CC(K)
      WRITE(6,506)
      WRITE(6,406)
      DO 76 K=1,10
      N=K-1
   76 WRITE(6,501) N,CH(K)
C
C                CONSIDER ICE FORMATION AT A POINT  -  Z
C
C                   ------
C
C                CALCULATE STEADY STATE ICE THICKNESS
C
      CALL RPF(Z,GAM,PETA,RS,RP)
      IF(RS.EQ.1.0) GO TO 90
      WRITE(6,106)
      WRITE(6,107) RS,BI,Z
      WRITE(6,104) CICE,CH2O,PR,PMU,TC,TL,TF,RHO
C
C                SOLVE THE DIFFERENTIAL EQUATION FOR
C                INTERFACE HISTORY BY FORWARD INTEGRATION
C
C                   ------
C
C
C                COMMENCE RUNGE KUTTA ------------------------
C
      H=0.01
      N=1
      R(N,1)=0.0
      R(N,2)=R(N,1)+H/2.0
```

```
      R(N,3)=R(N,1)+H/2.0
      R(N,4)=R(N,1)+H
      T(N)=0.0
      RR=(1.0-RP*R(N,1))
      WRITE(6,109) R(N,1),T(N),RR
      X(N)=R(N,1)
      Y(N)=T(N)
      DO 1 M=1,4
      XX(M)=1.0-RP*R(N,M)
    1 TP(N,M)=XX(M)*(GAM-ALOG(XX(M)))/((1.0-BETA*(GAM-ALOG(X
     *   X(M))))*RP)
      DELT(N)=(H/6.0)*(TP(N,1)+(2.0*TP(N,2))+(2.0*TP(N,3))+T
     *   P(N,4))
      DO 2 N=2,100
      R(N,1)=R(N-1,1)+H
      R(N,2)=R(N,1)+H/2.0
      R(N,3)=R(N,1)+H/2.0
      R(N,4)=R(N,1)+H
      T(N)=T(N-1)+DELT(N-1)
      DO 3 M=1,4
      XX(M)=1.0-RP*R(N,M)
    3 TP(N,M)=XX(M)*(GAM-ALOG(XX(M)))/((1.0-BETA*(GAM-ALOG(X
     *   X(M))))*RP)
      DELT(N)=(H/6.0)*(TP(N,1)+(2.0*TP(N,2))+(2.0*TP(N,3))+T
     *   P(N,4))
      RR=(1.0-RP*R(N,1))
      WRITE(6,109) R(N,1),T(N),RR
      X(N)=R(N,1)
    2 Y(N)=T(N)
C
C                END RUNGE KUTTA ------------------------------
C
      IF(KONST.EQ.1) GO TO 90
C
C                BEGIN PLOT ROUTINE
C
      CALL PLOTS(DATA(1),4096)
      CALL PLOT (0.0,0.0,23)
      CALL PLOT(0.0,12.5,3)
      CALL PLOT(6.0,12.5,2)
      CALL PLOT(0.0,0.0,3)
      CALL SCALE (X,6.0,100,1,20.0)
      CALL SCALE (Y,8.0,100,1,20.0)
      CALL AXIS (0.0,0.0,21HRADIUS (RO-R)/(RO-RS),-21,6.0,0.
     *   0,X(101),X(1
     02),20.0)
      CALL AXIS (0.0,0.0,19HDIMENSIONLESS  TIME,19,8.0,90.0,
     *   Y(101),Y(102
     2),20.0)
      CALL LINE(X,Y,100,1,0,0)
      CALL DRAW1(RS,ZCRIT,Z)
      CALL PLOT(0.0,0.0,3)
      CALL PLOT(12.0,0.0,23)
```

```
      WRITE(6,106)
      WRITE(6,300)((X(K),Y(K)),K=1,100)
   90 I=0
C
C              CALCULATE AND PLOT AXIAL PROFILES
C              OF RADIUS AND PRESSURE
C
      MOP=MZ*100
      BIGZ=FLOAT(MOP)*0.001
      CALL PRESS1(BIGZ,TIME)
      WRITE(6,301) TIME,RO
      DO 4 M=MR,MT,MZ
      I=I+1
      ZZ=FLOAT(M)*0.001
      X(I)=ZZ
      Y(I)=DELZ(ZZ,TIME)
      WRITE(6,300) X(I),Y(I)
      IF(I.EQ.100) GO TO 5
    4 CONTINUE
    5 IF(KONST.EQ.1) GO TO 202
      CALL SCALE(X,8.0,100,1,20.0)
      CALL SCALE(Y,6.0,100,1,20.0)
      CALL AXIS(0.0,0.0,20HDIMENSIONLESS LENGTH,-20,8.0,0.0,
     *  X(101),X(102
     1),20.0)
      CALL AXIS(0.0,0.0,20H   RADIUS  (R/RO)    ,20,6.0,90.0,
     *  Y(101),Y(102
     1),20.0)
      CALL LINE(X,Y,100,1,0,0)
      CALL DRAW2(TIME,ZCRIT)
      CALL PLOT(0.0,0.0,3)
      WRITE(6,106)
      WRITE(6,300)((X(K),Y(K)),K=1,100)
      CALL PLOT(0.0,14.0,23)
  202 WRITE(6,302) TIME,RO
      DO 6 I=1,100
      RR=Y(I)
      W(I)=PRESS(PP,RR,I)
    6 WRITE(6,300) X(I),W(I)
      IF(KONST.EQ.1) GO TO 200
      CALL SCALE(W,6.0,100,1,20.0)
      CALL SCALE(X,8.0,100,1,20.0)
      CALL AXIS(0.0,0.0,20HDIMENSIONLESS LENGTH,-20,8.0,0.0,
     *  X(101),X(102
     1),20.0)
      CALL AXIS(0.0,0.0,23HDIMENSIONLESS PRESSURE ,23,6.0,90
     *  .0,W(101),W(
     1102),20.0)
      CALL LINE(X,W,100,1,0,0)
      CALL DRAW2(TIME,ZCRIT)
      CALL PLOT(0.0,0.0,3)
      CALL PLOT(12.0,-14.0,3)
      CALL PLOT (0.0,0.0,999)
```

```
C
C              END PLOT ROUTINE
C
      WRITE(6,106)
      WRITE(6,300)((X(K),W(K)),K=1,100)
  100 FORMAT('0',10X,'SINCE ''ZCRIT'' IS LESS THAN 0.001 THE
     *   BLOCK PROFI
     1LE  TL = ',F6.2,' IS THEN INPUT INTO THE ICE PROBLEM')
  101 FORMAT(I2)
  102 FORMAT(5F6.3,F6.2,2F6.3)
  104 FORMAT('0',5X,'CONSTANTS     KI = ',F4.2,', KL = ',F6.3
     *  ,', PP = ',F
     F6.3,', MU = ',F6.3,', TC = ',F6.2,', TL = ',F6.2,', TF
     *   = ',F6.2,',
     6 RHO = ',F6.3/)
  105 FORMAT(3F8.3,F12.6,F12.6)
  106 FORMAT('1')
  107 FORMAT('0',2X,'   ICE INTERFACE POSITION AND TIME FOR
     *    RS/RO = ',
     2F8.6,10X,'ROHO/K = ',F7.3,10X,'Z* = ',F7.4)
  109 FORMAT(' ',10X,' POSITION RO-R/RO-RS = ',F6.4,10X,'DIM
     *  ENSIONLESS
     3TIME =  ',F9.6,10X,'R/RO = ',F6.4)
  300 FORMAT(' ',F6.4,F12.6)
  301 FORMAT('1',' Z        R/RO',10X,'TIME = ',F7.4,' HRS
     *  ,      RO = '
     1,F6.3,' FT.'/)
  302 FORMAT('1',' Z        PRESSURE',10X,'TIME = ',F7.4,' H
     *  RS,      RO =
     1 ',F6.3,' FT.'/)
  403 FORMAT(' ',10X,I2,10X,F10.6,10X,F10.6)
  405 FORMAT('1',10X,'N',12X,'EIGENVALUE',15X,'C(N)'//)
  406 FORMAT('0',10X,'N',10X,'-1/2C(N)R''(1)'//)
  500 FORMAT('0',10X,'I',10X,'EIGENVALUE'//)
  501 FORMAT(' ',10X,I2,10X,F10.6)
  504 FORMAT('0',10X,'I',10X,'CK(I)'//)
  506 FORMAT('0')
  507 FORMAT('0',10X,'FREEZING TEMPERATURE CHECK  TF = ',F7.
     *  3)
  508 FORMAT('0',10X,'EIGENVALUES FOR THE ICE FREE ZONE')
  509 FORMAT(' ',10X,'FOR ''BIOT'' NO. = ',F8.3/)
  510 FORMAT('0',10X,'BLOCK INLET TEMPERATURE PROFILE = ',F6
     *  .2//)
  511 FORMAT('0',30X,'CYLINDRICAL ICE FORMATION WITH CONVECT
     *  IVE BOUNDARY
     1 CONDITIONS'//)
  600 FORMAT('0',10X,'ICE WILL NOT FORM UNTIL ''Z/RO*RE*PR''
     *   = ',F8.6)
  700 FORMAT(F7.4,3I4)
  900 FORMAT(2I3,7F7.3)
  901 FORMAT('0',25X,'R/RO  VS.  (T-TF)/(TL-TF)  AT THE INLE
     *  T TO THE ICE
     1 PROBLEM'/)
```

```
902 FORMAT('0',10X,'------------------>   (T-TF)/(TL-TF)')
200 STOP
    END
```

```
      FUNCTION PRESS(PR,RR,I)
      COMMON BIOT,TE,TC,TL,CICE,CH2O,BI
      COMMON RLAM(40),RLAMW(40),CH(40),CC(40),CK(40),RLR(100
     *  1)
      COMMON RTR(101,40),PRES(101),VA(101)
      SS=PRES(I+1)
      RSQ=RR*RR
      CON=(4.0/3.0)*(1.0-RSQ*RSQ)/(RSQ*RSQ)
      PRESS=CON+32.0*PR*SS
      RETURN
      END
```

```
      FUNCTION DELZ(Z,TQ)
      DIMENSION XX(4),TP(1001,4),DELT(1001),R(1001,4),T(1001
     *   )
      COMMON BIOT,TF,TC,TL,CICE,CH2O,BI
      COMMON RLAM(40),RLAMW(40),CH(40),CC(40),CK(40),RLR(100
     *   1)
      COMMON RTP(101,40),PRES(101),VA(101)
      COMMON CLI,RHOI,RO
      H=0.001
      CALL RPF(Z,GAM,BETA,RS,RP)
      IF(RS.EQ.1.0) GO TO 23
      THETAC=TF-TC
      TCONST=(CLI/THETAC)*RHOI*RP*RP*RO*RO/CICE
      TZ=TQ/TCONST
      N=1
      R(N,1)=0.0
      R(N,2)=R(N,1)+H/2.0
      R(N,3)=R(N,1)+H/2.0
      R(N,4)=R(N,1)+H
      T(N)=0.0
      TEST=T(N)
      IF(TEST.GE.TZ) GO TO 20
      DO 1 M=1,4
      XX(M)=1.0-RP*R(N,M)
    1 TP(N,M)=XX(M)*(GAM-ALOG(XX(M)))/((1.0-BETA*(GAM-ALOG(X
     *   X(M))))*RP)
      DELT(N)=(H/6.0)*(TP(N,1)+(2.0*TP(N,2))+(2.0*TP(N,3))+T
     *   P(N,4))
      DO 2 N=2,1000
      R(N,1)=R(N-1,1)+H
      R(N,2)=R(N,1)+H/2.0
      R(N,3)=R(N,1)+H/2.0
      R(N,4)=R(N,1)+H
      T(N)=T(N-1)+DELT(N-1)
      TEST=T(N)
      IF(TEST.GE.TZ) GO TO 22
      DO 3 M=1,4
      XX(M)=1.0-RP*R(N,M)
    3 TP(N,M)=XX(M)*(GAM-ALOG(XX(M)))/((1.0-BETA*(GAM-ALOG(X
     *   X(M))))*RP)
    2 DELT(N)=(H/6.0)*(TP(N,1)+(2.0*TP(N,2))+(2.0*TP(N,3))+T
     *   P(N,4))
      GO TO 21
   22 ROB=R(N-1,1)
      TOB=T(N-1)
      H=0.000001
      N=1
      R(N,1)=ROB
      R(N,2)=R(N,1)+H/2.0
      R(N,3)=R(N,1)+H/2.0
      R(N,4)=R(N,1)+H
      T(N)=TOB
      DO 5 M=1,4
```

```
      XX(M)=1.0-RP*R(N,M)
    5 TP(N,M)=XX(M)*(GAM-ALOG(XX(M)))/((1.0-BETA*(GAM-ALOG(X
     *   X(M))))*RP)
      DELT(N)=(H/6.0)*(TP(N,1)+2.0*TP(N,2)+2.0*TP(N,3)+TP(N,
     *   4))
      DO 6 N=2,1000
      R(N,1)=R(N-1,1)+H
      R(N,2)=R(N,1)+H/2.0
      R(N,3)=R(N,1)+H/2.0
      R(N,4)=R(N,1)+H
      T(N)=T(N-1)+DELT(N-1)
      TEST=T(N)
      IF(TEST.GE.TZ) GO TO 20
      DO 7 M=1,4
      XX(M)=1.0-RP*R(N,M)
    7 TP(N,M)=XX(M)*(GAM-ALOG(XX(M)))/((1.0-BETA*(GAM-ALOG(X
     *   X(M))))*RP)
    6 DELT(N)=(H/6.0)*(TP(N,1)+2.0*TP(N,2)+2.0*TP(N,3)+TP(N,
     *   4))
      GO TO 21
   20 DELZ=(1.0-RP*R(N,1))
      RETURN
   21 DELZ=RS
      RETURN
   23 DELZ=1.0
      RETURN
      END
```

```
      FUNCTION RLNP(RLAMD,K)
      PI=3.1415926
      KK=K-1
      RK=FLOAT(KK)
      PLMIN=SIN((RK+1.0+0.5)*PI)
      X=(2.0**0.666667)/(3.0**0.833333)
      RLNP=(PLMIN*X*(RLAMD**0.333333))/GAMMA(1.333333)
      RETURN
      END
```

```
      SUBROUTINE VALUE(ZCRIT)
      COMMON BIOT,TF,TC,TL,CICE,CH2O,BI
      COMMON RLAM(40),RLAMW(40),CH(40),CC(40),CK(40),RLR(100
     *  1)
      COMMON RTR(101,40),PRES(101),VA(101)
      IF(TL.EQ.TF) GO TO 2
      IF(ZCRIT.LT.1.0E-3) GO TO 2
      THETAF=TC-TF
      THETAI=TL-TC
      DO 3 K=1,100
      SUM=0.0
      DO 1 J=1,40
      RLAW=RLAMW(J)
      ERP=RLAW*RLAW*ZCRIT
      IF(ERP.GE.174.673) GO TO 50
      GO TO 51
   50 CHIP=0.0
      GO TO 52
   51 CHIP=CK(J)*RTR(K,J)*EXP(-ERP)
      ACHP=ABS(CHIP)
      IF(ACHP.LT.1.0E-20) GO TO 55
   52 SUM=SUM+CHIP
    1 CONTINUE
   55 VALUE1=SUM
      VA(K)=(THETAF+THETAI*VALUE1)/(THETAF+THETAI)
    3 CONTINUE
      VA(101)=0.0
      RETURN
    2 CONTINUE
      DO 4 K=1,101
      VA(K)=1.0
    4 CONTINUE
      RETURN
      END
```

```
      SUBROUTINE PRESS1(BIGZ,TZ)
      COMMON BIOT,TF,TC,TL,CICE,CH2O,RI
      COMMON RLAM(40),RLAMW(40),CH(40),CC(40),CK(40),RLR(100
     *  1)
      COMMON RTR(101,40),PRES(101),VA(101)
      DIMENSION TP(101,4),DELT(101),Z(101,4)
      H=BIGZ/100.0
      N=1
      Z(N,1)=0.0
      Z(N,2)=Z(N,1)+H/2.0
      Z(N,3)=Z(N,1)+H/2.0
      Z(N,4)=Z(N,1)+H
      PRES(N)=0.0
      DO 1 M=1,4
      X=Z(N,M)
      DELPR=DELZ(X,TZ)
      DELSQD=DELPR*DELPR
      TP(N,M)=1.0/(DELSQD*DELSQD)
    1 CONTINUE
      DELT(N)=(H/6.0)*(TP(N,1)+2.0*TP(N,2)+2.0*TP(N,3)+TP(N,
     *  4))
      DO 2 N=2,101
      Z(N,1)=Z(N-1,1)+H
      Z(N,2)=Z(N,1)+H/2.0
      Z(N,3)=Z(N,1)+H/2.0
      Z(N,4)=Z(N,1)+H
      PRES(N)=PRES(N-1)+DELT(N-1)
      DO 3 M=1,4
      X=Z(N,M)
      DELPR=DELZ(X,TZ)
      DELSQD=DELPR*DELPR
      TP(N,M)=1.0/(DELSQD*DELSQD)
    3 CONTINUE
      DELT(N)=(H/6.0)*(TP(N,1)+2.0*TP(N,2)+2.0*TP(N,3)+TP(N,
     *  4))
    2 CONTINUE
      RETURN
      END
```

```
      SUBROUTINE RLN(RLAMD)
      DIMENSION R(1002,4),RR(1002,4),RRP(1002,4),RRPP(1002,4
     *   ),DELR(1002)
     1,DELRP(1002)
      COMMON BIOT,TF,TC,TL,CICE,CH2O,BI
      COMMON RLAM(40),RLAMW(40),CH(40),CC(40),CK(40),RLR(100
     *   1)
      COMMON RTR(101,40),PRES(101),VA(101)
      H=0.001000
      N=1
      R(N,1)=0.0
      RR(N,1)=1.0
      RRP(N,1)=0.0
      RRPP(N,1)=0.0
      R(N,2)=R(N,1)+H/2.0
      RR(N,2)=RR(N,1)+RRP(N,1)*H/2.0
      RRP(N,2)=RRP(N,1)+RRPP(N,1)*H/2.0
      RRPP(N,2)=(RLAMD*RLAMD*R(N,2)*(R(N,2)*R(N,2)-1.0)*RR(N
     *   ,2)-RRP(N,2)
     1)/R(N,2)
      R(N,3)=R(N,1)+H/2.0
      RR(N,3)=RR(N,1)+RRP(N,2)*H/2.0
      RRP(N,3)=RRP(N,1)+RRPP(N,2)*H/2.0
      RRPP(N,3)=(RLAMD*RLAMD*R(N,3)*(R(N,3)*R(N,3)-1.0)*RR(N
     *   ,3)-RRP(N,3)
     1)/R(N,3)
      R(N,4)=R(N,1)+H
      RR(N,4)=RR(N,1)+RRP(N,3)*H
      RRP(N,4)=RRP(N,1)+RRPP(N,3)*H
      RRPP(N,4)=(RLAMD*RLAMD*R(N,4)*(R(N,4)*R(N,4)-1.0)*RR(N
     *   ,4)-RRP(N,4)
     1)/R(N,4)
      DELR(N)=(H/6.0)*(RRP(N,1)+2.0*RRP(N,2)+2.0*RRP(N,3)+RR
     *   P(N,4))
      DELRP(N)=(H/6.0)*(RRPP(N,1)+2.0*RRPP(N,2)+2.0*RRPP(N,3
     *   )+RRPP(N,4))
      RLR(N)=RR(N,1)
      DO 1 N=2,1001
      R(N,1)=R(N-1,1)+H
      RR(N,1)=RR(N-1,1)+DELR(N-1)
      RRP(N,1)=RRP(N-1,1)+DELRP(N-1)
      RRPP(N,1)=(RLAMD*RLAMD*R(N,1)*(R(N,1)*R(N,1)-1.0)*RR(N
     *   ,1)-RRP(N,1)
     1)/R(N,1)
      R(N,2)=R(N,1)+H/2.0
      RR(N,2)=RR(N,1)+RRP(N,1)*H/2.0
      RRP(N,2)=RRP(N,1)+RRPP(N,1)*H/2.0
      RRPP(N,2)=(RLAMD*RLAMD*R(N,2)*(R(N,2)*R(N,2)-1.0)*RR(N
     *   ,2)-RRP(N,2)
     1)/R(N,2)
      R(N,3)=R(N,1)+H/2.0
      RR(N,3)=RR(N,1)+RRP(N,2)*H/2.0
      RRP(N,3)=RRP(N,1)+RRPP(N,2)*H/2.0
```

```
      RRPP(N,3)=(RLAMD*RLAMD*R(N,3)*(R(N,3)*R(N,3)-1.0)*RR(N
     *   ,3)-RRP(N,3)
     1)/R(N,3)
      R(N,4)=R(N,1)+H
      RR(N,4)=RR(N,1)+RRP(N,3)*H
      RRP(N,4)=RRP(N,1)+RRPP(N,3)*H
      RRPP(N,4)=(RLAMD*RLAMD*R(N,4)*(R(N,4)*R(N,4)-1.0)*RR(N
     *   ,4)-RRP(N,4)
     1)/R(N,4)
      DELR(N)=(H/6.0)*(RRP(N,1)+2.0*RRP(N,2)+2.0*RRP(N,3)+RR
     *   P(N,4))
      DELRP(N)=(H/6.0)*(RRPP(N,1)+2.0*RRPP(N,2)+2.0*RRPP(N,3
     *   )+RRPP(N,4))
      RLR(N)=RR(N,1)
    1 CONTINUE
      RETURN
      END
```

```
      SUBROUTINE RPF(Z,GAM,BETA,RS,RP)
      COMMON BIOT,TF,TC,TL,CICE,CH20,BI
      COMMON RLAM(40),RLAMW(40),CH(40),CC(40),CK(40),RLR(100
     *  1)
      COMMON RTR(101,40),PRES(101),VA(101)
      IF(Z.EQ.0.0) GO TO 13
      CHI=0.0
      DO 76 K=1,40
      RLAMD=RLAM(K)
      ERP=RLAMD*RLAMD*Z
      IF(ERP.GE.174.673) GO TO 50
      GO TO 57
   50 CHAPS=0.0
      GO TO 52
   57 CHAPS=CH(K)*EXP(-ERP)
      ACPIK=ABS(CHAPS)
      IF(ACPIK.LT.1.0E-20) GO TO 55
   52 CHI=CHI+CHAPS
   76 CONTINUE
   55 IF(TL.EQ.TF) GO TO 81
      TT=(TF-TC)/(TL-TF)
      GAM=1.0/BI
      BB=(TT*CICE)/(2.0*CH20*CHI)
      BETA=1.0/BB
      X=GAM-BB
      IF(X) 11,12,12
   11 Y=ABS(X)
      IF(Y.GE.174.673) GO TO 58
      RS=EXP(X)
  111 CONTINUE
      RP=1.0-RS
      GO TO 10
   81 RS=0.0
      GAM=1.0/BI
      BETA=0.0
      GO TO 111
   58 RS=0.0
      GO TO 111
   12 RS=1.0
      WRITE(6,100) X
      GO TO 111
   13 RS=1.0
      GO TO 111
   10 RETURN
  100 FORMAT('+',100X,'ARG. X = ',E9.6)
      END
```

```
      SUBROUTINE FUNC(X,GOFX,GPRIMX)
      COMMON BIOT,TF,TC,TL,CICF,CH2O,RI
      PI=3.1415926
      CONST=((3.0**0.666667)*GAMMA(1.333333))/((2.0**0.33333
     *   33)*GAMMA(0.
     3666667))
      S1=SIN((X*PI/4.0)-(PI/3.0))
      S2=SIN((X*PI/4.0)-(2.0*PI/3.0))
      C1=COS((X*PI/4.0)-(PI/3.0))
      C2=COS((X*PI/4.0)-(2.0*PI/3.0))
      GOFX=(1.0/BIOT)+((CONST*S2)/(S1*(X**0.6666667)))
      RIMX=((S1*C2)-(S2*C1))/(S1*S1)
      Y=-(2.0/3.0)*(S2/(S1*(X**1.666667)))
      Z=(PI/4.0)*RIMX/(X**0.6666667)
      GPRIMX=CONST*(Y+Z)
      RETURN
      END
```

```
      SUBROUTINE TRANS1(X,EPSLON,M)
C
C     ..............ROOT FINDER FOR TRANSCENDENTAL EQUATIONS
C
C     ..............USAGE
C                     -----
C                     CALL TRANS1(ROOT,ACCRCY,ITERNS)
C
C     ..............FUNC IS A USER SUPPLIED SUBROUTINE THAT
C     ..............CALCULATES F(X) AND F'(X).
C
C     ..............ENTRY TRANS1
C                     ------------
C     ..............FIND A REAL ROOT OF THE REAL-VALUED
C     ..............TRANSCENDENTAL EQUATION F(X)=0.
C                     ROOT......INITIAL GUESS AND CALCULATED
C                               ZERO
C                     ACCRCY....ITERATION BOUND
C                               X(I+1)-X(I)<EPSLON
C                     ITERNS....MAXIMUM NUMBER OF ITERATIONS
C
      XPP=X
      CALL FUNC(XPP,YPP,YDPP)
      XP=XPP-YPP/YDPP
      DO 2 I=1,M
      CALL FUNC(XP,YP,YDP)
      D=XP-XPP
      IF(ABS(D).LT.2.98E-08) GO TO 24
      A=(3.0*YDP+YDPP-3.0*(YP-YPP)/D)/D
      U=YP/YDP
      X=XP-U*(1.0+U*A/YDP)
      IF(ABS((X-XP)/X)-EPSLON)3,3,4
    4 XPP=XP
      XP=X
      YPP=YP
    2 YDPP=YDP
      WRITE(6,22)
   22 FORMAT(' FAILURE--INCREASE M AND/OR INCREASE EPSLON')
    5 STOP
   24 WRITE(6,23)
   23 FORMAT(' FAILURE--ACCURACY REQUIREMENTS EXCEED S.P. SI
     *  GNIFICANCE')
    3 RETURN
      END
```

```
      SUBROUTINE NUMER4(A,B,SS4)
      COMMON BIOT,TF,TC,TL,CICF,CH20,BI
      COMMON PLAM(40),RLAMW(40),CH(40),CC(40),CK(40),RLR(100
     *  1)
      COMMON RTR(101,40),PRES(101),VA(101)
      F(C)=C*(1.0-C*C)
      N2=100
      N3=N2/2
      H=(B-A)/FLOAT(N2)
      M1=IFIX(A*1000.0)+1
      M2=IFIX((A+H)*1000.0)+1
      S=F(A)*RLR(M1)+4.0*F(A+H)*RLR(M2)
      N1=N3-1
      DO 1 I=1,N1
      M3=IFIX((A+H*FLOAT(2*I))*1000.0)+1
      M4=IFIX((A+H*FLOAT(2*I+1))*1000.0)+1
      S=2.0*F(A+H*FLOAT(2*I))*RLR(M3)+4.0*F(A+H*FLOAT(2*I+1)
     *  )*RLR(M4)+S
    1 CONTINUE
      M5=IFIX(B*1000.0)+1
      X=F(B)*RLR(M5)+S
      SS4=H*X/3.0
      RETURN
      END
```

```
      SUBROUTINE INTEG1(A,B,SS1)
      COMMON BIOT,TE,TC,TL,CICE,CH2O,BI
      COMMON RLAM(40),RLAMW(40),CH(40),CC(40),CK(40),RLR(100
     *  1)
      COMMON RTR(101,40),PRES(101),VA(101)
      F(C)=C*(1.0-C*C)
      N2=100
      N3=N2/2
      H=(B-A)/FLOAT(N2)
      M1=IFIX(A*1000.0)+1
      M2=IFIX((A+H)*1000.0)+1
      S=F(A)*RLR(M1)*RLR(M1)+4.0*F(A+H)*RLR(M2)*RLR(M2)
      N1=N3-1
      DO 1 I=1,N1
      M3=IFIX((A+H*FLOAT(2*I))*1000.0)+1
      M4=IFIX((A+H*FLOAT(2*I+1))*1000.0)+1
      S=2.0*F(A+H*FLOAT(2*I))*RLR(M3)*RLR(M3)+4.0*F(A+H*FLOA
     *  T(2*I+1))*RL
     1R(M4)*RLR(M4)+S
    1 CONTINUE
      M5=IFIX(B*1000.0)+1
      X=F(B)*RLR(M5)*RLR(M5)+S
      SS1=H*X/3.0
      RETURN
      END
```

```
      SUBROUTINE INTEG2(A,B,SS2)
      COMMON BIOT,TF,TC,TL,CICE,CH2O,BI
      COMMON RLAM(40),RLAMW(40),CH(40),CC(40),CK(40),RLR(100
     *  1)
      COMMON RTR(101,40),PRES(101),VA(101)
      F(C)=C*(1.0-C*C)
      N2=100
      N3=N2/2
      H=(B-A)/FLOAT(N2)
      M1=IFIX(A*1000.0)+1
      N1=IFIX(A*100.0)+1
      M2=IFIX((A+H)*1000.0)+1
      N2=IFIX((A+H)*100.0)+1
      S=F(A)*RLR(M1)*VA(N1)+4.0*F(A+H)*RLR(M2)*VA(N2)
      N1=N3-1
      DO 1 I=1,N1
      M3=IFIX((A+H*FLOAT(2*I))*1000.0)+1
      N3=IFIX((A+H*FLOAT(2*I))*100.0)+1
      M4=IFIX((A+H*FLOAT(2*I+1))*1000.0)+1
      N4=IFIX((A+H*FLOAT(2*I+1))*100.0)+1
      S=2.0*F(A+H*FLOAT(2*I))*RLR(M3)*VA(N3)+4.0*F(A+H*FLOAT
     *  (2*I+1))*RLR
     1(M4)*VA(N4)+S
    1 CONTINUE
      M5=IFIX(B*1000.0)+1
      N5=IFIX(B*100.0)+1
      X=F(B)*RLR(M5)*VA(N5)+S
      SS2=H*X/3.0
      RETURN
      END
```

APPENDIX B

ORDER OF MAGNITUDE ANALYSIS OF THE GOVERNING EQUATIONS

Consider the governing differential equations: continuity, momentum, energy. For cylindrical coordinates assuming axi-symmetry, no sources, and negligible viscous energy dissipation.

Continuity:

$$\frac{d\rho}{dt} + \rho\left[\frac{\partial v_z}{\partial z} + \frac{1}{r}\frac{\partial}{\partial r}(rv_r)\right] = 0 \qquad \text{B-1}$$

Momentum:

$$\frac{\partial v_z}{\partial t} + v_z\frac{\partial v_z}{\partial z} + v_r\frac{\partial v_z}{\partial r} = -\frac{1}{\rho}\frac{\partial p}{\partial z} + \nu\left[\frac{\partial^2 v_z}{\partial r^2} + \frac{1}{r}\frac{\partial v_z}{\partial r} + \frac{\partial^2 v_z}{\partial z^2}\right] - g \qquad \text{B-2}$$

$$\frac{\partial v_r}{\partial t} + v_z\frac{\partial v_r}{\partial z} + v_r\frac{\partial v_r}{\partial r} = -\frac{1}{\rho}\frac{\partial p}{\partial r} + \nu\left[\frac{\partial^2 v_r}{\partial r^2} + \frac{1}{r}\frac{\partial v_r}{\partial r} + \frac{\partial^2 v_r}{\partial z^2} - \frac{v_r}{r^2}\right] \qquad \text{B-3}$$

Energy:

$$\frac{\partial^2\theta}{\partial r^2} + \frac{1}{r}\frac{\partial\theta}{\partial r} + \frac{\partial^2\theta}{\partial z^2} = \frac{1}{\alpha}\left[\frac{\partial\theta}{\partial t} + v_r\frac{\partial\theta}{\partial r} + v_z\frac{\partial\theta}{\partial z}\right] \qquad \text{B-4}$$

Consider the energy equation B-4. Normalizing we obtain

$$\left[\frac{\theta_c}{R_c^2}\right]\left[\frac{\partial^2\phi}{\partial R^2} + \frac{1}{R}\frac{\partial\phi}{\partial R}\right] + \left[\frac{\theta_c}{Z_c^2}\right]\frac{\partial^2\phi}{\partial Z^2} = \left[\frac{\theta_c}{\alpha t_c}\right]\frac{\partial\phi}{\partial\tau}$$

$$+ \left[\frac{\theta_c U_c}{\alpha R_c}\right] U\frac{\partial\phi}{\partial R} + \left[\frac{\theta_c V_c}{\alpha Z_c}\right] V\frac{\partial\phi}{\partial Z}$$

where $\phi = \frac{\theta}{\theta_c}$, $R = \frac{r}{R_c}$, $Z = \frac{z}{Z_c}$, $\tau = \frac{t}{t_c}$, $U = \frac{v_r}{U_c}$, $V = \frac{v_z}{V_c}$.

Multiplying the above equation by $\frac{1}{R_c^2}$ yields

$$\frac{\partial^2\phi}{\partial R^2} + \frac{1}{R}\frac{\partial\phi}{\partial R} + \left[\frac{R_c}{Z_c}\right]^2\frac{\partial^2\phi}{\partial Z^2} = \left[\frac{R_c^2}{\alpha t_c}\right]\frac{\partial\phi}{\partial\tau} + \left[\frac{U_c R_c}{\alpha}\right] U\frac{\partial\phi}{\partial R} + \left[\frac{V_c R_c^2}{Z_c}\right] V\frac{\partial\phi}{\partial Z}$$

or

$$\frac{\partial^2\phi}{\partial R^2} + \frac{1}{R}\frac{\partial\phi}{\partial R} + \left[\frac{R_c}{Z_c}\right]^2\frac{\partial^2\phi}{\partial Z^2} = \left[\frac{R_c^2}{\alpha t_c}\right]\frac{\partial\phi}{\partial\tau} + \left[\frac{V_c R_c^2}{\alpha Z_c}\right]\{V\frac{\partial\phi}{\partial Z} + \left[\frac{U_c Z_c}{V_c R_c}\right] U\frac{\partial\phi}{\partial R}\}.$$

If $\frac{\alpha t_c}{R_c^2} >> 1$, then the unsteady term is insignificant. Therefore

$$\frac{\partial^2\phi}{\partial R^2} + \frac{1}{R}\frac{\partial\phi}{\partial R} = \left[\frac{V_c R_c^2}{\alpha Z_c}\right]\{V\frac{\partial\phi}{\partial Z} + \left[\frac{U_c Z_c}{V_c R_c}\right] U\frac{\partial\phi}{\partial R}\}$$

where $R_c << Z_c$, i.e. the axial conduction is negligible. If advection is as important as the conduction terms, then $V_c R_c^2/\alpha Z_c = O(1)$. Hence

$$Z_c = \frac{R_c^2 V_c}{\alpha} = R_c Pr\ Re_{R_c}$$

The energy equation becomes

$$\frac{\partial^2\phi}{\partial R^2} + \frac{1}{R}\frac{\partial\phi}{\partial R} = \{V\frac{\partial\phi}{\partial Z} + [\frac{U_c Z_c}{V_c R_c}]\, U\frac{\partial\phi}{\partial R}\}. \qquad \text{B-5}$$

The solution of equation B-5 is valid for Z of O(1); however, the solution is expected to be accurate for smaller values of Z and therefore any solution will be extrapolated into this region.

Now consider the continuity equation but rewritten in the form

$$\frac{\partial\rho}{\partial t} + v_r\frac{\partial\rho}{\partial r} + v_z\frac{\partial\rho}{\partial z} + \rho[\frac{\partial v_z}{\partial z} + \frac{1}{r}\frac{\partial}{\partial r}(rv_r)] = 0 .$$

Normalizing we obtain

$$[\frac{\rho_c}{t_c}]\frac{\partial\rho'}{\partial\tau} + [\frac{\rho_c U_c}{R_c}]\, U\frac{\partial\rho'}{\partial R} + [\frac{\rho_c V_c}{Z_c}]\, V\frac{\partial\rho'}{\partial Z}$$

$$+ [\frac{\rho_c V_c}{Z_c}]\,\rho'\frac{\partial V}{\partial Z} + [\frac{\rho_c U_c}{R_c}]\,\rho'\frac{\partial(RU)}{\partial R} = 0$$

where $$\rho' = \frac{\rho}{\rho_c} .$$

But if $$\nabla\rho = (\frac{d\rho}{d\theta})_p \nabla\theta = -\beta\rho\nabla\theta$$

then

$$\rho_c\frac{\partial\rho'}{\partial R} = -\beta\theta_c\rho_c\rho'\frac{\partial\phi}{\partial R} \quad \text{and} \quad \rho_c\frac{\partial\rho'}{\partial Z} = -\beta\theta_c\rho_c\rho'\frac{\partial\phi}{\partial Z}$$

where β is the coefficient of thermal expansion

and the normalized continuity equation becomes

$$\left[\frac{Z_c}{t_c V_c}\right] \frac{\partial \rho'}{\partial \tau} + \rho' \left\{\frac{\partial V}{\partial Z} + \left[\frac{U_c Z_c}{V_c R_c}\right] \frac{\partial (RU)}{\partial R}\right\}$$

$$= \beta\theta_c \left\{V \frac{\partial \phi}{\partial Z} + \left[\frac{U_c Z_c}{V_c R_c}\right] U \frac{\partial \phi}{\partial R}\right\} . \qquad \text{B-6}$$

For the unsteady term to be insignificant ,

$$\frac{t_c V_c}{Z_c} = \frac{t_c \alpha}{R_c^2} >> 1$$

as in the energy equation. For water under atmospheric pressure $(\beta\theta_c)_{max} << 1$ and the right hand side of equation B-6 is suppressed since the terms inside the brackets {} are of order O(1) as shown by the analysis of the energy equation. Since $\rho' = O(1)$

$$\frac{\partial V}{\partial Z} + \left[\frac{U_c Z_c}{V_c R_c}\right] \frac{\partial (RU)}{\partial R} = 0 \quad .$$

Taking $\frac{U_c Z_c}{V_c R_c} = O(1)$ we define $U_c = \left(\frac{R_c}{Z_c}\right) V_c$, therefore

$$\frac{\partial V}{\partial Z} + \frac{\partial (RU)}{\partial R} = 0. \qquad \text{B-7}$$

Next consider the momentum equations

let $$p(r,z) = p^o(z) + p'(r,z)$$

where p^o = hydrostatic pressure at an interface

p' = pressure departure from p^o .

Thus $$\frac{\partial p}{\partial z} = \frac{\partial p^o}{\partial z} + \frac{\partial p'}{\partial z}$$

or $$\frac{\partial p}{\partial z} = - \rho_w g + \frac{\partial p'}{\partial z} .$$

The axial momentum equation B-2 becomes

$$\frac{\partial v_z}{\partial t} + v_z \frac{\partial v_z}{\partial z} + v_r \frac{\partial v_z}{\partial r} = - \frac{1}{\rho} \frac{\partial p'}{\partial z}$$

$$+ \nu[\frac{\partial^2 v_z}{\partial r^2} + \frac{1}{r} \frac{\partial v_z}{\partial r} + \frac{\partial^2 v_z}{\partial z}] + g(\frac{\rho_w}{\rho} - 1) . \qquad \text{B-8}$$

By definition, the coefficient of thermal expansion is

$$\beta = \frac{1}{\rho} (\frac{\partial \rho}{\partial T})_p$$

or

$$\beta = - \frac{1}{\rho} (\frac{\rho_w - \rho}{T_w - T}) .$$

Therefore equation B-8 becomes

$$\frac{\partial v_z}{\partial t} + v_z \frac{\partial v_z}{\partial z} + v_r \frac{\partial v_z}{\partial r} = - \frac{1}{\rho} \frac{\partial p'}{\partial z} + \left[\frac{\partial^2 v_z}{\partial r^2} + \frac{1}{r} \frac{\partial v_z}{\partial r} + \frac{\partial^2 v_z}{\partial z^2}\right] + \beta g \theta$$

where $$\theta = T - T_w \quad .$$

Normalizing the momentum equations, we obtain

$$\left[\frac{V_c}{t_c}\right] \frac{\partial V}{\partial \tau} + \left[\frac{V_c^2}{Z_c}\right] V \frac{\partial V}{\partial Z} + \left[\frac{V_c U_c}{R_c}\right] U \frac{\partial V}{\partial R} =$$

$$- \left[\frac{P_c'}{\rho Z_c}\right] \frac{\partial P'}{\partial Z} + \left[\frac{\nu V_c}{R_c^2}\right] \left(\frac{\partial^2 V}{\partial R^2} + \frac{1}{R} \frac{\partial V}{\partial R}\right) + \left[\frac{\nu V_c}{Z_c^2}\right] \frac{\partial^2 V}{\partial Z^2} + \beta g \theta_c \phi$$

$$\left[\frac{U_c}{t_c}\right] \frac{\partial V}{\partial \tau} + \left[\frac{U_c V_c}{Z_c}\right] V \frac{\partial U}{\partial z} + \left[\frac{U_c^2}{R_c}\right] U \frac{\partial U}{\partial R} =$$

$$- \left[\frac{P_c'}{\rho R_c}\right] \frac{\partial P'}{\partial R} + \left[\frac{\nu U_c}{R_c^2}\right] \left(\frac{\partial^2 U}{\partial R^2} + \frac{1}{R} \frac{\partial U}{\partial R} - \frac{U}{R^2}\right) + \left[\frac{\nu U_c}{Z_c^2}\right] \frac{\partial^2 U}{\partial Z^2}$$

where $$P' = \frac{p'}{P_c'} \quad .$$

Taking the axial momentum equation and multiplying by $\frac{R_c^2}{\nu V_c}$, we obtain

$$\left[\frac{R_c^2}{\nu t_c}\right] \frac{\partial V}{\partial \tau} + \left[\frac{R_c^2 V_c}{\nu Z_c}\right] V \frac{\partial V}{\partial Z} + \left[\frac{R_c U_c}{\nu}\right] V \frac{\partial U}{\partial R} =$$

$$= - \left[\frac{P_c' R_c^2}{\rho \nu Z_c V_c}\right] \frac{\partial P'}{\partial Z} + \frac{\partial^2 V}{\partial R^2} + \frac{1}{R} \frac{\partial V}{\partial R} + \left[\frac{R_c}{Z_c}\right]^2 \frac{\partial^2 V}{\partial Z^2} + \frac{\beta g R_c^2 \theta_c}{\nu V_c} \phi \quad .$$

Since the pressure and viscous forces are important

$$\left[\frac{P_c' R_c^2}{\rho \nu Z_c V_c}\right] = O(1)$$

defining $$P_c' = \frac{\mu Z_c V_c}{R_c^2} \quad .$$

If the unsteady term is to be insignificant

$$\frac{t_c \nu}{R_c^2} >> 1$$

where $$\frac{t_c \alpha}{R_c^2} = \frac{t_c \nu}{R_c^2} \cdot \frac{1}{Pr} \quad .$$

For water Pr > 1, therefore if $\frac{\alpha t_c}{R_c^2} >> 1$ then $\frac{\nu t_c}{R_c^2} >> 1$. Hence if the energy equation is quasi-steady, so are the momentum and continuity equations.

The axial momentum equation then becomes

$$\left[\frac{R_c^2 V_c}{\nu Z_c}\right]\left[V \frac{\partial V}{\partial Z} + U \frac{\partial V}{\partial R}\right] = - \frac{\partial P}{\partial Z} + \frac{\partial^2 V}{\partial R^2} + \frac{1}{R} \frac{\partial V}{\partial R} + \left[\frac{1}{PrRe}\right]^2 \frac{\partial^2 V}{\partial Z^2} + \left[\frac{Gr}{Re}\right]_{R_c} \phi$$

where $$Gr_{R_c} = \frac{\beta g R_c^3 \theta_c}{\nu^2} \quad , \quad \text{Grashof number}$$

$$Re_{R_c} = \frac{V_c R_c}{\nu} \quad , \text{ Reynolds number} \quad .$$

Therefore if $\frac{1}{PrRe} << 1$, i.e. axial conduction negligible, the equation reduces to

$$\left[\frac{1}{Pr}\right]\left[V\frac{\partial V}{\partial Z}+U\frac{\partial V}{\partial R}\right]=-\frac{\partial P'}{\partial Z}+\frac{\partial^2 V}{\partial R^2}+\frac{1}{R}\frac{\partial V}{\partial R}+\left[\frac{Gr}{Re}\right]_{R_c}\phi \qquad \text{B-9}$$

Normalizing the radial momentum equation B-3, we obtain

$$\left[\frac{1}{Pr}\right]\left[\frac{1}{PrRe}\right]^2\left[U\frac{\partial U}{\partial R}+V\frac{\partial U}{\partial Z}\right]=-\frac{\partial P'}{\partial R}$$

$$+\left[\frac{1}{PrRe}\right]^2\left[\frac{\partial^2 U}{\partial R^2}+\frac{1}{R}\frac{\partial U}{\partial R}-\frac{U}{R^2}\right]+\left[\frac{1}{PrRe}\right]^4\frac{\partial^2 U}{\partial Z^2}\,.$$

Again, since $\frac{1}{PrRe} << 1$ then

$$\frac{\partial P'}{\partial R}=0\,. \qquad \text{B-10}$$

The governing equations will now be applied to the ice-free and freezing zones.

A. Ice-Free Zone

Taking $R_c = r_0$ and $V_c = \frac{Q}{\pi r_0^2}$ equation B-5 becomes

$$\frac{\partial^2 \Phi_\ell}{\partial R^2}+\frac{1}{R}\frac{\partial \Phi_\ell}{R}=V\frac{\partial \Phi_\ell}{\partial Z}$$

remembering the flow is fully developed and $\frac{U_c Z_c}{V_c R_c} = O(1)$ from continuity. Since the advective terms are as important as the conduction terms

$$Z_c = r_0\, Pr\, Re_{ro}$$

The unsteady term in the energy equation was neglected although $\frac{t_c \alpha_\ell}{r_0^2} \geq 1$ experimentally. The tacit neglect of the unsteady term in the energy equation reveals that the solution for the temperature distribution in the ice-free zone is a steady state approximation.

Since the flow is fully developed hydrodynamically and if natural convection is negligible i.e.

$$Re_{ro} >> Gr_{ro}$$

where $$Gr_{ro} = \frac{\beta g r_0^3 \theta_c}{\nu^2}$$

and $$\theta_c = (T_\ell - T_w)_{max} = (T_\ell - T_c)[\Phi_\ell(0,z^+) - \Phi_\ell(1,z^+)]_{max}$$

then the momentum equation would reduce to

$$\frac{\partial^2 V}{\partial R^2} + \frac{1}{R}\frac{\partial V}{\partial R} = \frac{\partial P'}{\partial Z} \quad .$$

B. Freezing Zone

1. Liquid Phase

Taking $R_c = r_0$ and $V_c = \frac{Q}{\pi r_0^2}$ the energy equation becomes

$$\frac{\partial^2 \phi_\ell}{\partial R^2} + \frac{1}{R}\frac{\partial \phi_\ell}{\partial R} = V\frac{\partial \phi_\ell}{\partial Z} + U\frac{\partial \phi_\ell}{\partial R} \qquad \text{B-11}$$

Consider the energy balance at the ice-water interface

$$- k_\ell \left.\frac{\partial T_\ell}{\partial r}\right|_\delta - \rho_i L_i \frac{d\delta}{dt} = - k_i \left.\frac{\partial T_i}{\partial r}\right|_\delta .$$

Normalization reveals

$$\left[\frac{k_\ell}{k_i}\ \sigma\right] \left.\frac{\partial \phi_\ell}{\partial R}\right|_\Delta + \left[\frac{\rho_i L_i R_c^{\,2}}{k_i \theta_{ci} t_c}\right] \frac{d\Delta}{d\tau} = \left.\frac{\partial \phi_i}{\partial R}\right|_\Delta \qquad \text{B-12}$$

where $\sigma = \dfrac{\theta_{c\ell}}{\theta_{ci}}$, the superheat ratio

$$\Delta = \frac{\delta}{R_c}$$

$$R = \frac{r}{R_c} .$$

For a growing layer of ice, the coefficient of the middle term of equation B-12 cannot be very small without suppressing the nature of the problem, ice formation, therefore consider this coefficient of order O(1). The significance of the heat flux in the water depends on the coefficient $\frac{k_\ell}{k_i}\sigma$; for the experimental cases this term is of the order (10^{-1}). This indicates that the exclusion of the unsteady term in the energy equation has only a small effect on the solution for the interface history.

Considering the axial momentum equation, the inertia terms are insignificant when $Pr \gg 1$ ($Pr = 13.6$ for freezing water) and natural convection is negligible if $Re_{ro} \gg Gr_{ro}$, where

$$\theta_c = (T_{\ell} - T_f)_{max} = [\phi_{\ell}(0,z^*)(T_0 - T_f) - T_f]_{max} .$$

2. Solid Phase

Consider the energy equation as given by equation B-4; we obtain after normalization

$$\frac{\partial^2 \phi_i}{\partial R^2} + \frac{1}{R}\frac{\partial \phi_i}{\partial R} + \left[\frac{R_c}{Z_c}\right]^2 \frac{\partial^2 \phi_i}{\partial Z^2} = \left[\frac{R_c^2}{t_c \alpha_i}\right] \frac{\partial \phi_i}{\partial \tau} .$$

Consider Z_c equal to the frozen length of the tube, i.e. $Z_c = \ell$, and $R_c = r_0$ then axial conduction in the ice is negligible if $r_0/\ell << 1$, yielding

$$\frac{\partial^2 \phi_i}{\partial R^2} + \frac{1}{R}\frac{\partial \phi_i}{\partial R} = \left[\frac{r_0^2}{t_c \alpha_i}\right] \frac{\partial \phi_i}{\partial \tau} . \qquad \text{B-13}$$

As demonstrated previously, by normalizing the equation for the energy balance at the solid-liquid interface an expression for t_c is found, such that equation B-13 takes the form

$$\frac{\partial^2 \phi_i}{\partial R^2} + \frac{1}{R}\frac{\partial \phi_i}{\partial R} = \text{Ste} \frac{\partial \phi_i}{\partial \tau} .$$

If Ste << 1, the unsteady term is negligible and the solution is "quasi-steady".

If the ice-water interface has reached a steady-state value the equation is simply

$$\frac{\partial^2 \phi_i}{\partial R^2} + \frac{1}{R}\frac{\partial \phi_i}{\partial R} = 0 .$$

$$\frac{\partial u}{\partial t} + \frac{1}{2}\frac{\partial u^2}{\partial x} = 0$$